

See discussions, stats, and author profiles for this publication at: <http://www.researchgate.net/publication/280631082>

# Connecting Groundwater and Surface Water Sources in Groundwater Dependent Coastal Wetlands and Estuaries: Sian Ka'an Biosphere Reserve, Quintana Roo, Mexico

ARTICLE *in* ESTUARIES AND COASTS · SEPTEMBER 2015

Impact Factor: 2.54 · DOI: 10.1007/s12237-014-9892-4

---

READS

111

6 AUTHORS, INCLUDING:



[David Lagomasino](#)

Florida International University

11 PUBLICATIONS 15 CITATIONS

[SEE PROFILE](#)



[René M. Price](#)

Florida International University

71 PUBLICATIONS 510 CITATIONS

[SEE PROFILE](#)



[Jorge Herrera Silveira](#)

Center for Research and Advanced Studies ...

98 PUBLICATIONS 753 CITATIONS

[SEE PROFILE](#)



[Fernando Miralles-Wilhelm](#)

University of Maryland, College Park

71 PUBLICATIONS 996 CITATIONS

[SEE PROFILE](#)

*Connecting Groundwater and Surface  
Water Sources in Groundwater Dependent  
Coastal Wetlands and Estuaries: Sian  
Ka'an Biosphere Reserve, Quintana Roo,  
Mexico*

**David Lagomasino, René M. Price, Jorge  
Herrera-Silveira, Fernando Miralles-  
Wilhelm, Gonzalo Merediz-Alonso &  
Yadira Gomez-Hernandez**

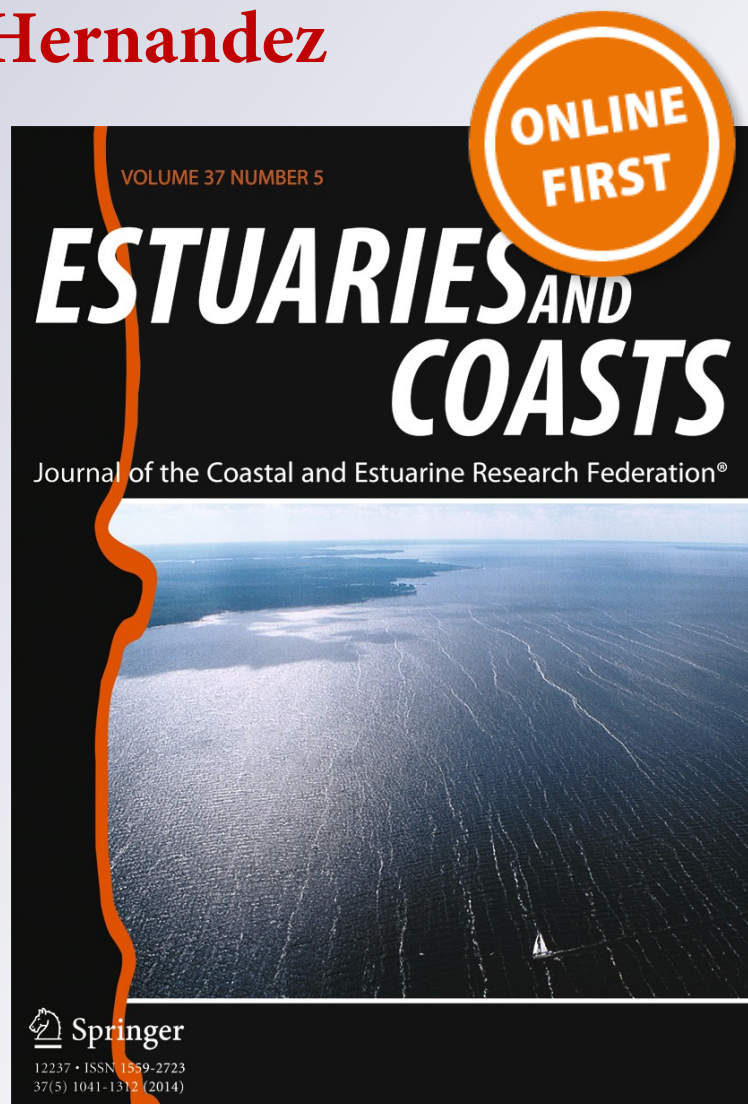
**Estuaries and Coasts**

Journal of the Coastal and Estuarine  
Research Federation

ISSN 1559-2723

Estuaries and Coasts

DOI 10.1007/s12237-014-9892-4



**Your article is protected by copyright and all rights are held exclusively by Coastal and Estuarine Research Federation. This e-offprint is for personal use only and shall not be self-archived in electronic repositories. If you wish to self-archive your article, please use the accepted manuscript version for posting on your own website. You may further deposit the accepted manuscript version in any repository, provided it is only made publicly available 12 months after official publication or later and provided acknowledgement is given to the original source of publication and a link is inserted to the published article on Springer's website. The link must be accompanied by the following text: "The final publication is available at [link.springer.com](http://link.springer.com)".**

# Connecting Groundwater and Surface Water Sources in Groundwater Dependent Coastal Wetlands and Estuaries: Sian Ka'an Biosphere Reserve, Quintana Roo, Mexico

David Lagomasino · René M. Price ·  
Jorge Herrera-Silveira · Fernando Miralles-Wilhelm ·  
Gonzalo Merediz-Alonso · Yadira Gomez-Hernandez

Received: 13 June 2014 / Revised: 20 August 2014 / Accepted: 12 September 2014  
© Coastal and Estuarine Research Federation 2014

**Abstract** Groundwater and surface water samples were collected in five different regions of the Sian Ka'an Biosphere Reserve (SKBR) along the eastern coast of the Yucatan Peninsula in Quintana Roo, Mexico. Samples were analyzed for major ions, total phosphorus, total nitrogen,  $\delta^{18}\text{O}$ , and  $\delta^2\text{H}$ . Chemical modeling and a coupled principal component analysis and end-member mixing model were used to identify three groundwater sources that discharge to the coastal wetlands and estuaries of the SKBR. A sulfate-dominated and a calcium-dominated fresh groundwater source were found to contribute significantly to the headwaters of a southern and northern SKBR estuary, respectively. In the northern part of the Reserve, an elevated road disrupts the flow of freshwater

through the estuarine zone creating hypersaline conditions and mangrove dead-zones. In a more pristine estuary to the south, coastal groundwater discharge associated with petens (tree islands) accounted for ~20 % of the surface water in the mid-estuary. This coastal groundwater discharge from the petens adds a significant amount of phosphorus to the surface water in the estuary relative to the upstream and downstream sources. The lower alkalinity measured in the surface water relative to the high-alkalinity groundwater, despite clear indication of groundwater discharge, suggests that inorganic carbon export through degassing of  $\text{CO}_2$  could represent important carbon process in mangrove ecosystems. Our results indicate an important groundwater discharge mechanism that may facilitate nutrient delivery to karstic, oligotrophic estuaries when upland and marine nutrient supplies are depleted.

Communicated by Nancy L. Jackson

D. Lagomasino (✉) · R. M. Price · F. Miralles-Wilhelm  
Department of Earth and Environment, Florida International  
University, Miami, FL, USA  
e-mail: david.lagomasino@nasa.gov

D. Lagomasino · R. M. Price  
Southeast Environmental Research Center, Florida International  
University, Miami, FL, USA

J. Herrera-Silveira  
CINVESTAV-IPN, Unidad Mérida, Carretera Antigua a Progreso  
km. 6, 97310 Mérida, Yucatán, Mexico

G. Merediz-Alonso  
Amigos de Sian Ka'an, Calle Fuego #2, 77500 Cancún, Quintana  
Roo, Mexico

Y. Gomez-Hernandez  
Comisión Nacional de Áreas Naturales Protegidas, Calle Vendado  
#71 & 72, 77500 Cancún, Quintana Roo, Mexico

## Present Address:

D. Lagomasino  
Universities Space Research Association, NASA Goddard Space  
Flight Center, Greenbelt, MD, USA

**Keywords** Groundwater discharge · Oligotrophic ·  
Eutrophic · Phosphorus · Mangroves · Hypersaline

## Introduction

Karst systems are groundwater dependent ecosystems (GDE) that rely heavily on groundwater to maintain their structure and functionality (Murray et al. 2003; Eamus and Froend 2006). The Yucatan peninsula is a highly karstified region that has limited surface water flow (Perry et al. 2003). Coastal wetlands are common environments along the coastline of the Yucatan and are important transition zones connecting terrestrial and aquatic GDEs that help to transfer material, energy and contaminants (Vervier et al. 2002). Alterations to the timing, quality, quantity, and distribution of groundwater by natural or anthropogenic means can potentially alter both the form and function of the GDE, the coastal wetlands and the shallow coastal waters (Murray et al. 2003; Foster et al. 2003).

Besides being an important driver and link for sustaining floral and faunal biodiversity in a wide variety of aquatic, terrestrial, and coastal environments, GDEs and particularly wetlands provide a myriad of ecosystem services for urban and agricultural development and expansion, recreation and other intangible benefits based upon social, cultural, and ethical considerations (Foster and Chilton 2003; Murray et al. 2003).

Coastal wetlands in karst regions can be heavily influenced by the temporal variability of groundwater discharge and groundwater quality from upstream sources (Halse et al. 2003; Gondwe et al. 2011) and coastal groundwater discharge (Price et al. 2006). For instance, groundwater discharge in a coastal mangrove estuary in South Africa has been shown to persist through seasons of drought, contributing to the resilience of the estuary (Taylor et al. 2006). Additionally, groundwater has been evidenced to deliver nutrients, particularly phosphorus, to coastal mangroves in Brazil and Florida through coastal groundwater discharge (Ovalle et al. 1990; Price et al. 2006). Continued urban and agricultural development along the coast and in the peninsular interior can lead to both physical (e.g., water flow) and chemical (e.g., nutrient loading) changes to the hydrology leading to eutrophication as seen in other estuaries of the peninsula that are located near urban centers (Herrera-Silveira et al. 2002).

Identifying subsurface water flow sources and pathways is important for understanding the links between GDEs and terrestrial and aquatic ecosystems (Eamus and Froend 2006). Various techniques (i.e., isotopic, chemical, and dye tracers) have been used to define water sources, measure water flow pathways, and quantify the contribution from each water source (Christophersen and Hooper 1992; Doctor et al. 2006; Price et al. 2006). Natural geochemical tracers have been used in combination with a principal component analysis (PCA) and end-member mixing analysis have been used in a variety of GDEs such as mountain stream catchments (Hooper et al. 1990; Liu et al. 2004; Abesser et al. 2006); lowlands (Baker and Vervier 2004; Garrett et al. 2012); wetlands (Vulava et al. 2008); and in karst terrains (Doctor et al. 2006).

A better understanding of the water flow pathways connecting GDEs is needed to help conserve and protect these important environments from the pressures of urban growth and development (Metcalfé et al. 2011). This knowledge may be particularly important in karst systems such as the Yucatan Peninsula, where there is little surface water flow but an intricate maze of caves, faults, and fractures for large amounts of groundwater to flow. Groundwater recharge areas in the peninsula interior and groundwater discharge points along the central coast are largely unidentified in the area. In addition, the wet season-dry season hydrodynamics in terms of coastal groundwater discharge and chemistry are poorly understood. Previous research has explored groundwater pathways in the geologically complex region of the mid and central Yucatan, though they have been limited to the peninsular interior (Perry et al. 2002, 2009; Marfia et al. 2004). This study expands upon previous

geochemical research conducted in the eastern Yucatan by investigating the fate and transport of water from the peninsular interior through the mangroves and estuaries of the Sian Ka'an Biosphere Reserve (SKBR). The objective of this study was to (1) measure the fate and transport of fresh water from inland to the coast through the wetlands and estuaries of the SKBR and (2) identify areas of coastal groundwater discharge to the Reserve.

## Study Area

The SKBR was established in 1986. Shortly thereafter, SKBR was declared a World Natural Heritage Site by UNESCO, was included on the Ramsar List of Wetlands of International Importance, and was the first project for the International Corporate Wetlands Restoration Partnership. At approximately 1.3 million acres (5280 km<sup>2</sup>), SKBR is the largest protected area in the Mexican Caribbean. The reserve is located on the eastern coast of the Yucatan peninsula, just south of the tourist destination of Tulum (Fig. 1). The reserve contains an extraordinary range of biodiversity as it encompasses the transition zone between upland tropical forests and savannas containing freshwater wetlands, lagoons, and cenotes (sinkholes) with marine coral reefs via brackish coastal mangrove wetlands and estuaries, the largest of which is the Bahia de Ascension (Fig. 1). Coastal wetlands along the eastern boundary of the SKBR are composed of a mixture of mangrove communities ranging in structure from dwarf to tall forms that are primarily dominated by *Rhizophora mangle* (Adame et al. 2013). Hammocks or petens (tree islands) also occur in the freshwater and brackish water wetlands. These concentric formations tend to occur around cenotes (Zaldívar-Jiménez et al. 2010) and consist of taller hardwoods, palms, or mangrove trees at the center radiating out to small trees, grasses, or dwarf mangroves.

Seasonal rains fall to the ground and then flow mostly underground through semi-deciduous forests, into an extensive freshwater-saltwater transitional wetland and ultimately, discharges into the Bahia de la Ascension. During the rainy season (mid-May to October), a majority of the annual rainfall (0.8–1.5 m) falls over the catchment (Olmstead and Duran 1990). Evapotranspiration rates are poorly constrained in the area, but initial estimates range from 40 to 85 % of the mean annual precipitation (Lesser 1976; Beddows 2004).

The Yucatan platform is ~150,000 km<sup>2</sup> and composed primarily of highly permeable carbonate rock (e.g., limestone, dolomite, carbonate-rich impact breccia), with over 1-km thick sequences along the coast and thinning toward the center of the peninsula (Ward et al. 1995). The carbonate platform is composed of a series of terraces, the oldest terrace (Eocene) is found in the center of the peninsula and the youngest (Holocene) formed along the coast (Ward 1985). The high porosity and permeability of the limestone bedrock and the lack of soils allow water to quickly recharge the aquifer,

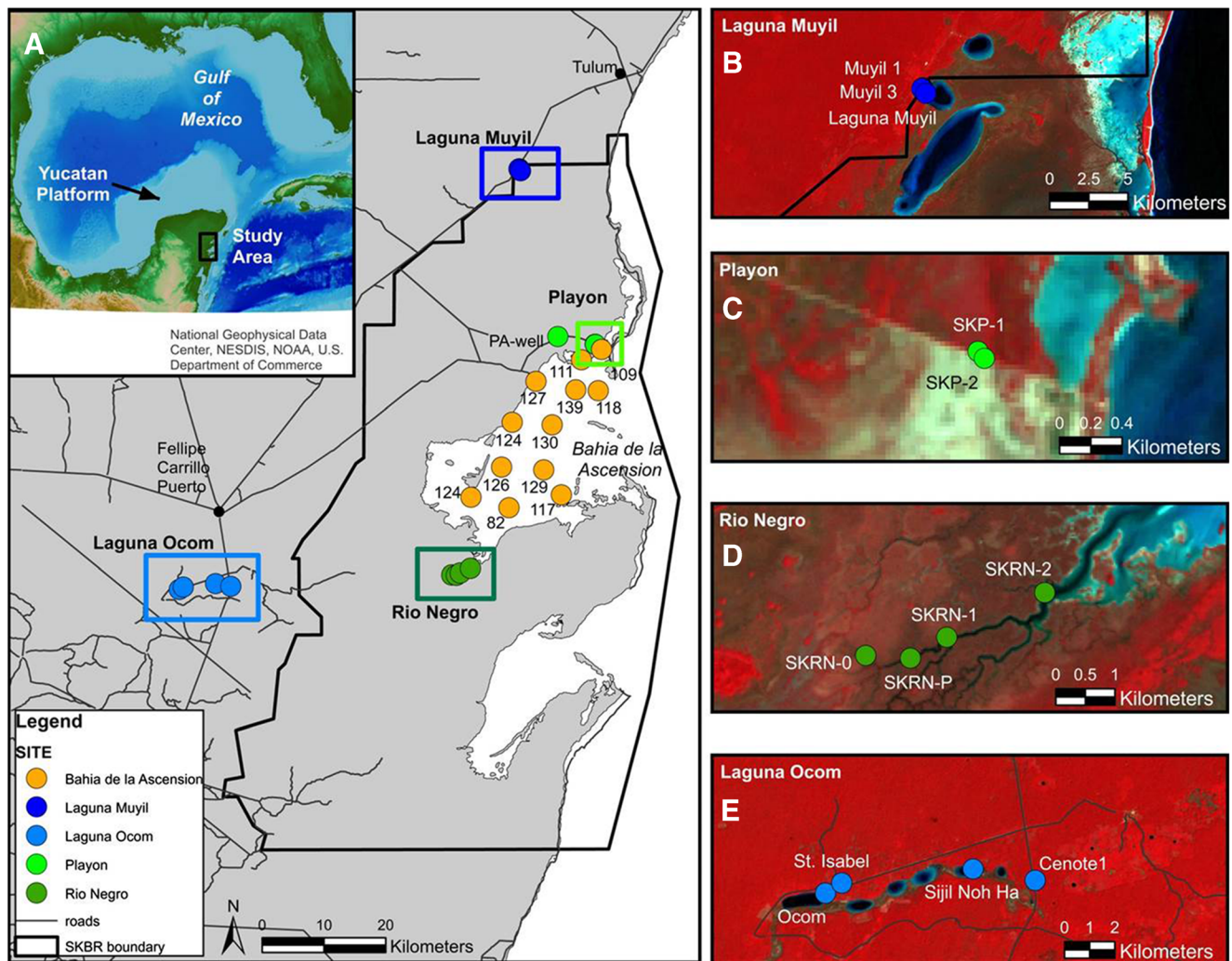


**Fig. 1** a Map of the Sian Ka'an Biosphere Reserve showing the locations of study sites in the Bahia de la Ascension, b Laguna Muyil, c Playon, d Rio Negro, e and Laguna Ocom. Circle markers indicate locations of

water samples in each of the respective sites. Site colors remain the same throughout the figures

resulting in the absence of surface streams (Beddows et al. 2007). Fractures, along with joints and bedding planes have been documented in nearby quarries and in flooded caverns and have created an extensive below-ground cavernous pathway allowing increased hydraulic conductivity and permeability (Beddows et al. 2007). Some dissolution features become exposed at the surface in the form of cenotes. The cenotes may extend ~100 m below the water table and may connect with horizontal dissolution features associated with multiple sea-level stands (Beddows 2004).

**Methods**

**Peat Groundwater Wells**

Groundwater wells were installed at six mangrove sites; two at Playon near the north end of the Bahia de Ascension and four

along the Rio Negro near the southern end of the Bahia de Ascension (Fig. 1). The two wells at the Playon site were installed in December 2010 and placed on either side of a road that transects through the mangrove zone. These two sites were designated as SKP-1 (north of the road) and SKP-2 (south of the road) (Figs. 1 and 2) and were installed in the peat sediments just above the top of the bedrock at a depth of ~1 m. The well north of the road, SKP-1, was located in a relatively pristine, natural mangrove environment, while south of the road has experienced high tree mangrove mortality since the construction of the road (Fig. 2). The four wells constructed at the Rio Negro site (e.g., SKRN-0, SKRN-P, SKRN-1, and SKRN-2) were installed approximately 4–5 m from the river channel and located 5, 4, 3.2, and 1.5 km from the mouth of Rio Negro, respectively. Two wells, SKRN-1 and SKRN-2, were installed in December 2010 and wells, SKRN-0 and SKRN-P, were installed in May 2012. The groundwater well at SKRN-P was located within a tall

**Fig. 2** Picture, facing west, of Playon showing the undisturbed mangrove site (SKP-1) to the right (north) of the road, and the disturbed mangrove site (SKP-2) to the left (south) of the road



mangrove peten (Adame et al. 2013), while the other five wells were installed among the dwarf mangroves. Each groundwater well was constructed from a 2.54-cm diameter PVC pipe consisting of a solid riser and a 42.9 cm long well screen at the base. Wells were placed in the center of a 10.2-cm diameter borehole excavated with a bucket auger. Once wells were placed in the borehole, coarse carbonate sand was poured into the borehole surrounding the well screen to approximately 7.5 cm above the well screen. A 10–12 cm layer of fine carbonate sand was placed on top of the coarse sand and then followed by a layer of Portland cement up to the ground surface. Each well was developed 24 h after installation by surging and pumping for at least 1 h to remove any fine-grained particulates that may have settled within the well and the coarse sand pack.

#### Water Samples

Surface water samples were collected in and along the coastal mangrove region of the SKBR including the Bahia de la Ascension (BA) estuary, as well as from cenotes at Laguna Muyil located at the northern end of the SKBR, and Laguna Ocom located approximately 11 km south of the town of Felipe Carrillo Puerto (Fig. 1). Water samples were collected at Playon, Rio Negro, and the Bahia de la Ascension during the end of the wet season in December 2010. These aforementioned sites were resampled at the end of the dry season in May 2012 along with the two inland freshwater sites at Laguna Muyil and Ocom (Table 1). Groundwater samples (GW) were collected from the six well sites (e.g., SKRN-0, SKRN-1, SKRN-P, SKRN-2, SKP-1, SKP-2) located at Rio Negro and El Playon. Those groundwater wells were first purged of three well volumes of water using a peristaltic pump before the sample was collected. Pore water samples were collected at 20 cm (PW-20) and 50 cm (PW-50) below the ground surface at each well site using an acrylic tube and syringe. The tube that contained small openings near the bottom was inserted into the soils to the appropriate depths; water samples were then collected through the tube via a syringe and then filtered. Surface water samples (SFW) and GW samples were collected using a peristaltic pump.

Groundwater was also collected from a water supply well (PA-well) located approximately 8 km inland of the coastline along the Playon road (Fig. 1) and from a small village well (St. Isabel) located near Laguna Ocom. The PA-well was

approximately 25 m deep and bored into the limestone bedrock. Water from this well was sampled from a discharge valve in the well pipe after discharging for several minutes. The water from the well located at St. Isabel was sampled via a bucket that was lowered down the well and then filtered. The water level in the well was approximately 8 m below the ground surface, though the depth of the well is unknown.

Salinity, water temperature, specific conductance, dissolved oxygen and pH were measured in the field using an Orion multi-probe and a Thermo Scientific three-start pH meter (accuracy  $\pm 0.02$ ) at the time of sample collection. Water samples collected from each source (e.g., GW, PW-20, PW-50, and SFW) consisted of a set of filtered and unfiltered samples. Unfiltered water samples were collected directly into dry, acid-washed bottles and acidified with a 10 % HCl solution to be analyzed for total nutrient concentrations of phosphorus (TP), nitrogen (TN), and organic carbon (TOC). Water samples collected for ionic concentrations (cations, anions, and alkalinity) and stable isotopes were filtered through a 0.45- $\mu\text{m}$  filter. Samples collected for cation analysis were acidified to a pH of less than 2 with 10 % HCl. All samples were placed on ice and kept refrigerated until they were ready for analysis. Major anion ( $\text{Cl}^-$  and  $\text{SO}_4^{2-}$ ) and cation ( $\text{Na}^+$ ,  $\text{K}^+$ ,  $\text{Mg}^{2+}$ , and  $\text{Ca}^{2+}$ ) analyses were completed in the Hydrogeology Laboratory at FIU using a Dionex 120 Ion Chromatograph. Stable isotope ratios of hydrogen ( $\delta^2\text{H}$ ) and oxygen ( $\delta^{18}\text{O}$ ) were measured on a DLT-1000 Liquid Water Isotope Analyzer (Los Gatos, Inc) with an accuracy of 0.6 and 0.2‰, respectively. Total alkalinity was determined on the water samples using a Brinkman Titrimo 751 Titrator with 0.1 N concentration of HCl to a pH of 2. Total alkalinity was calculated from the volume of acid added at the inflection point closest to a pH of 4. Change in volume of the sample due to the addition of the titrant was not considered. Total alkalinity was calculated as milliequivalents per liter  $\text{HCO}_3^-$ , as the pH of the water samples was near neutral. Duplicates of a small subset of water samples were analyzed to test the titrator precision which had standard deviations less than 0.25 meq  $\text{L}^{-1}$ .

Saturation indices (S.I.) of the water samples were determined with respect to the minerals calcite, aragonite, dolomite, anhydrite, and gypsum using the geochemical model PHREEQC version 2.14.2 (Parkhurst and Appelo 1999). Positive S.I. values ( $\text{S.I.} > 0$ ) indicated that the water sample was supersaturated with respect to that mineral and that mineral

**Table 1** Summary of water sampling sites, water types, field parameters, stable isotopes, major cation and anion concentrations, and nutrient concentrations collected in the Sian Ka'an Biosphere Reserve

Site	Station name	Water type	Date (mm/d/yy)	Temp (°C)	Conductivity (mS)	Salinity (psu)	D.O. (mg/L)	pH	$\delta^2\text{H}$ ‰	$\delta^{18}\text{O}$ ‰	Alkalinity (mmol L <sup>-1</sup> )	Cl <sup>-</sup> (mmol L <sup>-1</sup> )	SO <sub>4</sub> <sup>2-</sup> (mmol L <sup>-1</sup> )	Na <sup>+</sup> (mmol L <sup>-1</sup> )	K <sup>+</sup> (mmol L <sup>-1</sup> )	Mg <sup>2+</sup> (mmol L <sup>-1</sup> )	Ca <sup>2+</sup> (mmol L <sup>-1</sup> )	TN (μmol L <sup>-1</sup> )	TP (μmol L <sup>-1</sup> )	TOC (μmol L <sup>-1</sup> )
Playon	PA-well	GW	12/7/2010	25.3	1.303	0.6	6.26	7.62	-22.37	-4.32	4.4	7.9	0.2	6.0	0.1	0.8	2.1	22.37	0.13	278.08
	SKP-1	SFW	12/8/2010	24.9	5	2.7	8.47	7.8	5.70	0.25	6.1	44.4	0.5	33.7	0.7	3.8	2.2	45.96	0.14	1168.33
Rio Negro	SKP-1	GW	12/8/2010	24	10.48	5.9	0.21	6.55	1.54	-0.25	7.4	99.3	1.5	77.0	1.8	9.5	3.7	85.87	0.58	1622.50
	SKP-2	GW	12/8/2010	25.3	76.6	53.2	0.05	6.62	11.20	2.02	10.7	863.4	19.9	708.5	13.1	102.8	17.0	204.44	1.60	2032.50
Rio Negro	SKP-2	SFW	12/8/2010	29.4	19.83	11.7	6.2	a	a	a	a	a	a	a	a	a	a	a	a	a
	SW-2	SFW	12/7/2010	21.7	0	0.3	3.44	7.36	-7.77	-1.71	4.3	2.3	0.0	1.6	0.0	0.2	1.5	51.94	0.35	1672.50
Rio Negro	SKRN-0	SFW	12/8/2010	20.8	2.606	1.4	5.21	7.62	0.67	0.15	4.1	15.4	1.3	12.8	0.3	3.2	3.1	36.51	0.10	749.50
	SKRN-1	GW	12/9/2010	27.9	31.87	19.8	0.09	6.57	-0.08	-0.78	19.4	314.4	6.0	262.8	6.3	35.9	14.2	64.94	0.32	1920.83
Bahia de la Ascension	SKRN-1	SFW	12/9/2010	23.7	2.46	1.3	8.56	7.92	-0.25	-0.25	3.0	16.1	1.4	12.0	0.3	3.1	2.8	38.42	0.10	730.17
	SKRN-2	SFW	12/9/2010	24.1	3.97	2.1	8.66	8.07	-0.93	-0.86	3.1	32.2	1.5	23.9	0.5	4.3	2.9	41.05	0.11	847.50
Bahia de la Ascension	SKRN-81	SFW	12/9/2010	23.7	9.88	5.5	9.72	8.13	1.55	0.36	3.0	82.1	2.4	72.0	2.0	9.9	4.1	66.89	0.19	809.42
	SKRN-82	SFW	12/9/2010	23.7	35.14	22.1	8.36	8.36	0.71	-0.12	2.7	348.4	6.9	292.7	8.0	35.6	7.8	39.32	0.15	538.92
Bahia de la Ascension	SKP-109	SFW	12/9/2010	23.8	48.19	31.4	8.27	8.32	7.69	1.29	2.8	478.7	9.2	415.5	11.3	50.7	9.2	30.80	0.12	412.50
	SKP-111	SFW	12/9/2010	23.6	45.15	29.3	10.69	8.41	6.95	0.24	3.4	438.4	9.1	388.1	10.7	47.8	8.5	43.09	0.12	565.67
Playon	SK-Lagoon	SFW	12/9/2010	25.5	37.95	24.1	11.57	8.35	14.65	2.06	5.0	346.8	7.0	322.1	8.1	37.8	7.8	83.09	0.37	1187.50
	SKP-1	SFW	05/09/12	29	8.49	4.3	5.83	7.99	2.96	1.09	4.5	72.3	3.2	56.7	1.2	6.6	3.9	50.02	0.28	1789.67
Playon	SKP-1	20	05/09/12	30.1	9.97	5.6	0.88	7.48	4.19	1.29	5.0	89.6	4.0	73.5	1.6	8.7	4.5	83.53	0.47	1809.00
	SKP-1	50	05/09/12	31.7	20.49	12.1	0.93	7.33	6.75	1.32	9.0	229.8	10.4	205.0	5.0	27.1	8.9	142.18	1.67	3705.67
Playon	SKP-1	GW	05/09/12	30.2	14.41	8.3	0.92	7.61	8.87	1.69	5.3	141.6	7.0	114.3	2.6	13.7	5.4	94.09	0.64	2102.33
	SKP-2	SFW	05/09/12	31.9	55.9	36.9	5.81	8.55	22.93	4.00	3.4	396.1	21.8	481.5	12.7	57.3	13.0	128.75	0.32	2254.00
Playon	SKP-2	20	05/09/12	32	78.6	54.5	0.61	7.11	15.36	2.40	5.6	857.6	49.5	759.5	15.0	102.3	20.8	336.33	1.65	3500.83
	SKP-2	50	05/09/12	31	105	76.9	0.37	6.99	9.86	1.79	9.3	1110.3	65.3	957.9	21.1	131.0	22.8	580.89	4.53	3089.17
Rio Negro	SKP-2	GW	05/09/12	30.2	99.5	71.9	0.34	7.2	9.04	2.11	7.9	1043.1	61.7	892.1	19.5	114.5	23.4	502.50	3.02	2967.50
	SKRN-0	SFW	05/10/12	29.5	16.84	9.8	1.67	7.97	28.16	6.16	3.5	142.7	12.6	125.8	2.8	17.8	8.1	86.14	0.38	1678.00
Rio Negro	SKRN-0	20	05/10/12	31.1	17.63	10.7	3.2	7.36	21.89	4.26	6.6	158.9	12.0	142.7	3.1	19.4	9.0	a	a	a
	SKRN-0	50	05/10/12	29.7	22.33	13.3	2.27	6.84	-4.17	0.47	11.6	227.8	14.9	186.3	4.0	26.0	14.0	a	a	a
Rio Negro	SKRN-0	GW	05/10/12	29.6	25.45	15.5	0.76	6.9	2.51	1.45	10.8	247.5	15.8	203.9	4.7	27.6	12.7	76.01	0.85	1409.67
	SKRN-P	SFW	05/10/12	30.9	22.01	13.2	2.7	8.13	20.88	4.66	3.3	207.8	15.2	176.0	3.9	23.0	8.4	96.98	0.55	1497.33
Rio Negro	SKRN-P	20	05/10/12	27.6	39.97	25.5	0.25	6.45	6.23	0.53	11.2	430.9	32.7	344.4	6.5	49.8	21.8	a	a	a
	SKRN-P	50	05/10/12	28	43.37	27.5	0.5	6.47	-2.93	-0.56	13.5	456.5	36.8	361.8	8.2	54.0	24.2	a	a	a
Rio Negro	SKRN-P	GW	05/10/12	27.2	50.6	33	0.8	6.47	-3.53	-0.37	16.4	549.8	38.6	420.0	7.3	60.8	27.1	168.01	6.72	4564.67
	SKRN-1	SFW	05/10/12	32.4	29.05	17.7	4.2	8.15	20.02	3.93	3.2	225.9	14.6	201.7	6.0	25.7	7.9	52.90	0.75	1040.00
Rio Negro	SKRN-1	20	05/10/12	34.1	14.7	20	1.66	7.06	19.51	3.61	5.2	262.2	15.8	240.4	5.4	30.7	10.4	a	a	a
	SKRN-1	50	05/10/12	30.6	14.56	20	1.7	6.91	13.65	2.80	8.0	256.0	15.5	233.1	5.1	30.6	11.0	a	a	a
Rio Negro	SKRN-1	GW	05/10/12	29.2	34.07	21.3	0.78	6.86	-0.67	0.69	17.3	317.9	16.1	277.0	5.9	37.2	14.8	78.26	0.76	1921.00

**Table 1** (continued)

Site	Station name	Water type	Date (mm/d/yy)	Temp (°C)	Conductivity (mS)	Salinity (psu)	D.O. (mg/L)	pH	δ <sup>2</sup> H ‰	δ <sup>18</sup> O ‰	Alkalinity (mmol L <sup>-1</sup> )	Cl <sup>-</sup> (mmol L <sup>-1</sup> )	SO <sub>4</sub> <sup>2-</sup> (mmol L <sup>-1</sup> )	Na <sup>+</sup> (mmol L <sup>-1</sup> )	K <sup>+</sup> (mmol L <sup>-1</sup> )	Mg <sup>2+</sup> (mmol L <sup>-1</sup> )	Ca <sup>2+</sup> (mmol L <sup>-1</sup> )	TN (μmol L <sup>-1</sup> )	TP (μmol L <sup>-1</sup> )	TOC (μmol L <sup>-1</sup> )
	SKRN-2	SFW	05/10/12	34.4	37.55	23.5	5.55	8.44	20.36	4.38	3.0	368.6	21.4	307.1	8.2	38.8	11.0	80.18	0.57	1452.33
	SKRN-2	20	05/10/12	30.6	17.81	25	2.07	7.34	11.59	2.08	8.9	354.0	20.2	292.0	6.4	37.5	13.1	a	a	a
	SKRN-2	50	05/10/12	31.5	30.39	18.8	3	7.11	a	a	17.7	294.5	13.2	252.8	6.2	34.8	11.9	a	a	a
	SKRN-2	GW	05/10/12	29.1	11.65	6.6	1.5	6.84	a	a	10.6	96.0	7.8	84.1	2.3	11.7	9.9	21.63	0.29	262.57
Bahia De	SK-82	SFW	05/11/12	30	57.7	38.3	5.44	8.56	13.59	2.96	2.4	583.0	29.3	510.5	13.1	62.6	11.0	26.95	0.23	301.17
Ascension	SK-109	SFW	05/11/12	29.3	55.3	36.7	4.9	8.26	14.48	3.08	2.7	539.1	27.3	473.7	10.4	56.0	10.3	30.39	0.18	356.83
	SK-111	SFW	05/11/12	30.8	55.9	37	5.51	8.58	14.72	2.86	2.4	600.6	30.0	475.7	11.1	56.6	10.2	29.81	0.18	307.00
	SK-117	SFW	05/11/12	30.9	58.2	38.7	5.58	8.57	6.54	1.98	2.4	497.2	23.5	481.0	12.0	55.5	10.9	16.40	0.15	195.80
	SK-118	SFW	05/11/12	30.1	54.5	36	5.32	8.58	10.13	2.06	2.6	553.5	27.4	464.6	10.8	55.6	10.1	25.49	0.15	320.17
	SK-124	SFW	05/11/12	29.8	50.4	32.9	5.75	8.56	12.73	2.71	2.5	478.6	24.5	423.5	9.8	49.5	10.5	41.83	0.18	561.33
	SK-126	SFW	05/11/12	29.9	57	37.8	5.05	8.42	10.07	1.57	2.8	573.6	28.8	486.9	11.4	58.0	10.4	22.22	0.18	240.50
	SK-127	SFW	05/11/12	29.5	52.7	34.6	5.08	8.33	10.34	1.77	2.7	544.7	27.6	446.3	10.4	53.4	9.8	18.93	0.24	303.00
	SK-128	SFW	05/11/12	29.4	55	36.3	4.83	8.27	12.34	1.54	2.7	591.5	29.6	470.7	11.0	56.4	10.4	29.90	0.15	310.67
	SK-129	SFW	05/11/12	30	56.5	37.4	5.1	8.47	12.38	3.62	2.4	615.7	30.7	478.8	10.4	57.4	10.3	25.62	0.22	279.50
	SK-130	SFW	05/11/12	29.9	55.5	35.2	5.11	8.54	14.11	3.37	2.5	464.4	24.0	452.6	10.6	54.1	10.0	28.77	0.15	372.17
	SK-131	SFW	05/11/12	30.1	53.6	35.3	5.54	8.48	15.81	3.40	2.8	586.6	28.0	453.8	10.6	54.2	9.9	24.83	0.19	319.17
	SK-Lagoon	SFW	05/11/12	33.2	61.4	40.7	4.7	8.32	a	a	3.0	631.5	32.8	520.2	11.8	61.9	12.0	86.53	0.34	1179.00
Laguna	Ocom	Lagoon	05/12/12	29.4	15.4	0.8	5.65	8.26	9.69	2.82	2.9	6.0	3.1	6.3	0.2	2.4	2.1	31.13	0.14	412.50
Ocom	St Isabel	well	05/12/12	27.8	0.61	0.3	2.57	7.38	-22.45	-3.13	4.8	0.3	0.1	0.4	0.0	0.2	2.6	919.54	0.56	96.13
	Sijil	Cenote	05/12/12	26.5	1.745	0.9	0.06	7.03	-27.37	-5.17	7.0	3.7	4.2	4.3	0.1	2.5	5.0	127.07	0.49	120.93
	Ocom	Cenote	05/12/12	30.9	1.282	0.6	0.93	8.39	13.49	4.25	3.1	3.2	2.2	3.5	0.1	1.7	2.3	81.44	0.53	119.00
	Cenote1																			
Laguna	Muyil	Cenote	05/12/12	25.8	1.732	0.9	0.33	7.2	-24.63	-4.54	7.30	8.41	0.43	6.81	0.13	1.37	3.32	28.25	0.16	617.67
Muyil	Cenote1																			
	Muyil	Cenote	05/12/12	25.5	1.73	0.9	0.81	7.32	a	a	7.3	8.4	0.4	7.1	0.1	1.6	3.5	119.31	0.28	116.17
	Cenote3																			
Laguna	Muyil	Lagoon	05/12/12	a	a	0.7	a	a	-8.70	-1.78	3.3	7.8	0.4	6.4	0.1	1.5	1.2	50.70	0.23	295.67

a Missing data from samples

precipitation was most likely. Negative S.I. values ( $S.I. < 0$ ) indicated undersaturated conditions with respect to that mineral and that mineral dissolution was thermodynamically favored. Water samples with S.I. values near zero ( $\pm 0.05$ ) were considered to be at saturation (or at equilibrium) with respect to that mineral, and neither precipitation nor dissolution was expected to predominate. In addition to the saturation indices,  $\log p\text{CO}_2$  of the water samples were also determined using PHREEQC.

Total nutrient concentrations were determined at FIU's Southeast Environmental Research Center (SERC) water quality laboratory. Total phosphorus concentrations were determined using a dry ashing, acid hydrolysis technique developed by Solarzano and Sharp (1980). Total concentrations of nitrogen were analyzed on an ANTEK 7000N Nitrogen Analyzer that used  $\text{O}_2$  as a carrier gas instead of argon to promote complete recovery of the nitrogen in the water samples (Frankovich and Jones 1998). Total organic carbon concentrations were measured by direct injection onto hot platinum catalysis in a Shimadzu TOC-5000 after first acidifying to a pH of less than 2 and purging with  $\text{CO}_2$ -free air.

#### Principal Component Analysis and End-Member Mixing Model

Two PCAs were combined with an end-member analysis (EMMA) (Christophersen et al. 1990) to estimate the percent of the water contributed to each sample from a limited number of end-members. The titrator-measured alkalinity ( $\text{HCO}_3^-$ ), major anion ( $\text{Cl}^-$  and  $\text{SO}_4^{2-}$ ) and cation ( $\text{Na}^+$ ,  $\text{K}^+$ ,  $\text{Mg}^{2+}$ , and  $\text{Ca}^{2+}$ ) concentration data from the groundwater, pore water, and surface water samples were used in one PCA. The other PCA utilized the same chemical constituents but without total alkalinity. We included non-conservative tracer concentrations,  $\text{Ca}^{2+}$  and alkalinity, in the PCA as they were major ionic components of the water samples, and were used to identify mixing of groundwater with surface water. The PCA used an orthogonal transformation to convert the water chemistry data into various principal components, where the majority of the variance was explained by the first two principal components, U1 and U2. The eigenvectors of the U1 and U2 principal components made up the new transformed Euclidean space,  $U$  space. Water source end-members were determined by plotting the transformed data into  $U$  space according to the methods described in Christophersen and Hooper (1992). Once the end-members were identified, the proportions of each were determined by measuring the distance between each sample and each end-member in  $U$  space using the EMMA Microsoft EXCEL spreadsheet (available at [www.cof.orst.edu/cof/fe/watershed/Documents/Shortcourses/shortcourse/EMMA.xls](http://www.cof.orst.edu/cof/fe/watershed/Documents/Shortcourses/shortcourse/EMMA.xls)). Lastly, the predicted ionic concentrations modeled by the joint PCA-EMMA were then compared with the measured ionic concentrations to

determine the accuracy of the mixing model and to be sure the end-members were correctly identified. Further details and equations for the PCA and EMMA can be found in Christophersen and Hooper (1992).

## Results

### Water Chemistry

Salinity of the samples at the Playon sites ranged from 0.3 to 53.2 psu in December 2010 and 4.3 to 76.9 psu in May 2012 (Table 1). The lowest salinity values were obtained in water samples from the potable well (PA-well) and from the surface water cenote (SW-2). The highest salinity at Playon was measured in the PW-50 sample at SKP-2. Salinity values in the disturbed mangroves (SKP-2) were about an order of magnitude greater than salinities in the undisturbed mangroves (SKP-1) (Table 1). In general, groundwater and pore water samples had higher salinities and lower pH values ( $< 8$ ) than surface water at both Playon sites.

Salinities at Rio Negro ranged from 1.1 to 22.1 psu in December 2010 and from 6.6 to 35.6 psu in May 2012 (Table 1). Surface water salinities increased along a gradient from the most inland site (SKRN-0) to the mouth of the Rio Negro (SKRN-2). The groundwater from SKRN-2, located closest to the bay, had the lowest salinity relative to the other Rio Negro sites (Table 1). The highest salinities (30–36 psu) were measured in the groundwater and porewater sample in the peten at SKRN-P. The pH values of the groundwater and pore water samples were below 7.5 while surface water pH was generally above 8. In addition, pH gradually increased from the upstream site, SKRN-0, to the downstream site, SKRN-2.

The salinity in the Bahia de la Ascension ranged from 22.1 to 31.4 psu in December 2010 and from 32.9 to 40.7 psu in May 2012 (Table 1). Water samples were collected from more locations in the Bahia de la Ascension in December 2010 as compared to May 2012, especially in the center of the bay; therefore, the range of salinity during the December 2010 may not be representative of the entire bay. The pH values of the water in the Bahia de la Ascension ranged between 8.26 and 8.58, with the lowest pH values often observed along the coastline (Table 1). Samples from the freshwater cenotes generally had salinities less than 1. Water temperatures were around 25–26 °C for samples from cenotes (Sijil, Muyil Cenote1, and Muyil Cenote3) and relatively higher ( $> 27$  °C) for local wells (St. Isabel) and lagoon (Laguna Ocom) (Table 1). Two samples from Laguna Ocom (Ocom and Ocom Cenote1) had higher pHs ( $> 8.2$ ) than the other freshwater samples (Table 1). These samples were obtained closer to the surface and at a distance away from the spring discharge.

The surface water samples collected in the Bahia de la Ascension clustered tightly on a piper diagram as sodium chloride-type water (Fig. 3). The freshwater samples collected in the cenotes at Laguna Muyil and Laguna Ocom plotted in the center of the piper diagram with no particular dominant water type, but separate from one another with the Laguna Ocom samples containing slightly higher concentrations of sulfate (Fig. 3). Most of the groundwater, pore water, and surface water samples collected at Rio Negro and Playon were categorized as brackish water samples, defined as having a specific conductance greater than 5 mS cm<sup>-1</sup>. The water samples from Rio Negro plotted on the piper diagram as a mixture of seawater and freshwater from Laguna Ocom, while water samples from Playon plotted as a mixture of seawater and freshwater from Laguna Muyil (Fig. 3).

The δ<sup>18</sup>O and δ<sup>2</sup>H values of the surface water from the Bahia de la Ascension ranged from +1.29 to +3.62‰ and from +7.69 to +14.78‰, respectively. Stable isotope values were more variable in the surface waters at Rio Negro and Playon, ranging from -0.86 to +6.16‰ for δ<sup>18</sup>O and -3.47 to +28.16‰ for δ<sup>2</sup>H (Table 1). Freshwater samples collected from the inland cenotes exhibited more depleted isotopic values with δ<sup>18</sup>O values ranging from -5.17 to -1.78‰ and δ<sup>2</sup>H values from -27.37 to -8.70‰. On a plot of δ<sup>18</sup>O vs δ<sup>2</sup>H, all of the brackish to saline water samples plotted below the meteoric water line (MWL) along an evaporation line with a slope of 4.9 while the freshwater cenote samples plotted on the MWL, with the exception of two samples (Fig. 4). These two freshwater cenote samples collected from the Laguna Ocom

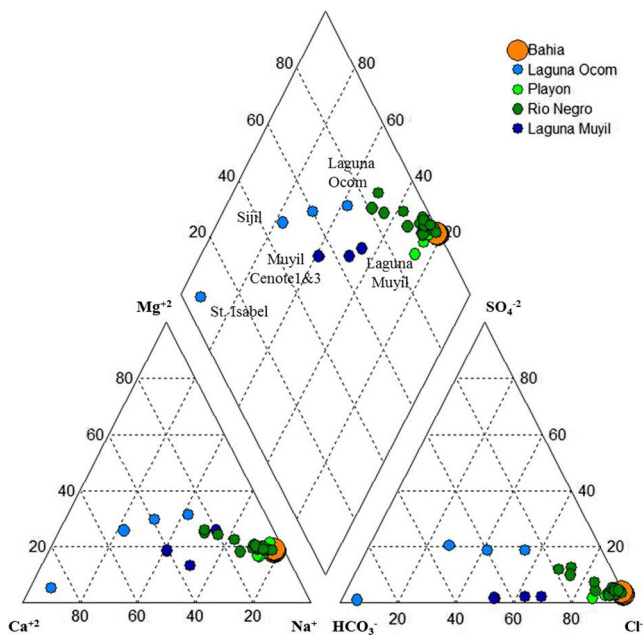


**Fig. 3** Piper diagram showing major ion chemistry of water samples collected in the Bahia de la Ascension, Laguna Ocom, Playon, Rio Negro, and Laguna Muyil

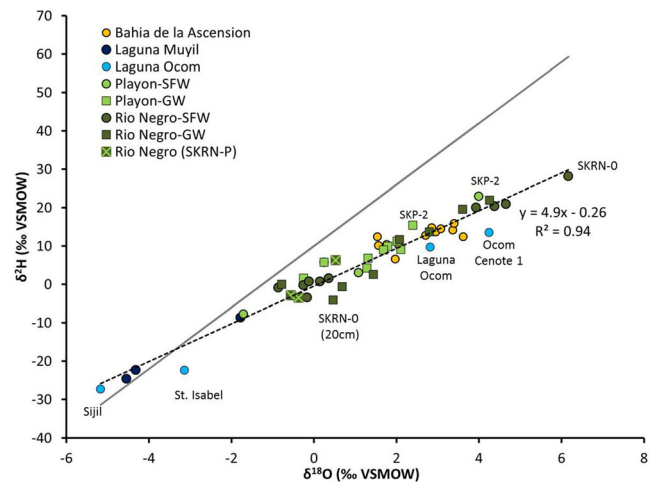


**Fig. 4** Plot of δ<sup>2</sup>H and δ<sup>18</sup>O for water samples collected at each site in the Sian Ka'an Biosphere reserve. The global meteoric water line (GMWL) is plotted as a gray line. The local evaporation line is plotted as a dotted black line

area (Laguna Ocom and Ocom Cenote 1) had enriched values of δ<sup>18</sup>O and δ<sup>2</sup>H, and plot higher along the evaporation line.

Groundwater isotopic signatures averaged +1.07‰ (δ<sup>18</sup>O) and +0.92‰ (δ<sup>2</sup>H) at the Rio Negro sites and +1.90‰ (δ<sup>18</sup>O) and +8.96‰ (δ<sup>2</sup>H) at the Playon sites (Fig. 4). The δ<sup>18</sup>O and δ<sup>2</sup>H values for the surface water averaged +4.82 and +22.84‰ at Rio Negro and +2.54 and +12.95‰ at Playon, respectively. Additionally, seasonal differences were identified between the December 2010 samples and the May 2012 samples (Table 1). December 2010 samples from Rio Negro and Playon were more depleted than the samples collected in May 2012 (Table 1). Samples collected in the Bahia de la Ascension exhibited similar seasonal isotopic variability, with more depleted values during December 2010 (Table 1).

Total phosphorus concentrations were typically lowest in fresh groundwater and in the brackish and saline surface water samples (Fig. 5). Freshwater collected from the inland cenotes

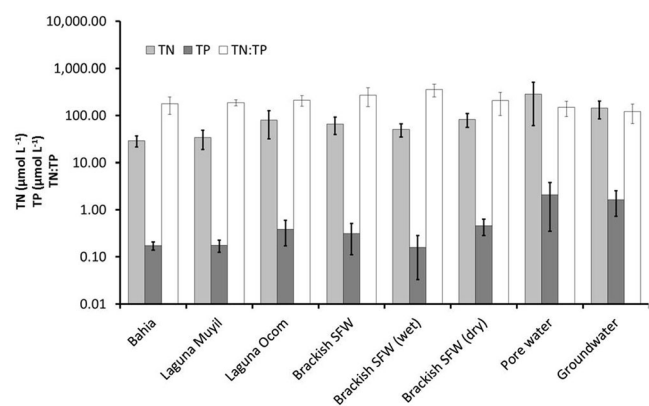


**Fig. 5** Concentrations (±1 standard deviation) of total nitrogen (TN), total phosphorus (TP) and TN:TP ratios plotted for samples from Bahia de la Ascension, Laguna Muyil, Laguna Muyil, brackish surface water from Playon and Rio Negro, pore water, and groundwater

had TP concentrations averaging  $0.39 \mu\text{mol L}^{-1}$  at Laguna Ocom and  $0.17 \mu\text{mol L}^{-1}$  (Fig. 5). Surface water TP concentrations in the brackish zone of Rio Negro and Playon ranged between  $0.09$  and  $0.75 \mu\text{mol L}^{-1}$  and averaged  $0.31 \mu\text{mol L}^{-1}$  (Table 1). Higher TP concentrations were observed in the Rio Negro and Playon surface water in May 2012 ( $0.46 \mu\text{mol L}^{-1}$ ) than in December 2010 ( $0.16 \mu\text{mol L}^{-1}$ ) (Table 1). Increasing surface water TP concentrations were observed along an estuarine gradient from  $\text{Cl}^-$  concentrations of  $\sim 15$  to  $200 \text{ mmol L}^{-1}$ , followed by a decrease in TP concentration beyond  $\text{Cl}^-$  concentrations of  $\sim 300 \text{ mmol L}^{-1}$  (Fig. 6a). The TP concentrations in the Bahia de la Ascension were lower than the brackish surface water in Rio Negro and Playon, and ranged between  $0.12$  and  $0.24 \mu\text{mol L}^{-1}$  with a mean concentration of  $0.17 \mu\text{mol L}^{-1}$  (Fig. 5). The highest average TP concentrations were observed in the pore water and groundwater at Rio Negro and Playon (Table 1 and Fig. 5). In particular, subsurface samples from SKRN-P at Rio Negro and SKP-2 at Playon had TP concentrations that exceeded  $1.6 \mu\text{mol L}^{-1}$  (Table 1).

The TN concentrations exhibited similar spatial variability as TP. Freshwater samples and surface water samples from the estuaries and Bahia de la Ascension tended to have lower TN concentrations. Total nitrogen (TN) concentrations were highly variable between the Laguna Ocom sites, with some of the

lowest TN concentrations ( $<50 \mu\text{mol L}^{-1}$ ) measured in the cenotes and the highest concentration ( $919.54 \mu\text{mol L}^{-1}$ ) measured at the St. Isabel well (Table 1; Fig. 6c). Groundwater and pore water samples generally had the highest average TN concentrations ranging from  $\sim 40$  to  $170 \mu\text{mol L}^{-1}$  (Table 1). Peak TN concentrations occurred in the subsurface samples at SKRN-P and SKP-2 (Table 1; Fig. 6). Surface water TN concentrations followed a similar estuarine gradient as the TP concentrations (Fig. 6b).

Concentrations of TOC shared similar patterns as TP and TN (Figs. 5 and 6b). Likewise, the TOC concentrations varied with  $\text{Cl}^-$  concentrations though the increases in TOC at lower  $\text{Cl}^-$  concentrations were not as pronounced as TP and TN (Fig. 6c). Water from the Bahia de la Ascension and the fresh groundwater from Laguna Ocom, and Laguna Muyil had the lowest TOC concentrations, ranging between  $116$  and  $617 \text{ mmol L}^{-1}$  (Table 1). Pore water and groundwater had the highest concentrations of TOC ( $>949 \text{ mmol L}^{-1}$ ) at SKRN-P and SKP-2 (Fig. 6b).

Surface water samples generally had the highest TN/TP ratios, ranging between  $\sim 150$  and  $425$  at the fresh groundwater sites (Laguna Ocom and Laguna Muyil) and between  $\sim 70$  and  $470$  in all surface water samples collected among Rio Negro, Playon, and Bahia de la Ascension (Figs. 5 and 6d). Surface water collected during December 2010 at Rio Negro

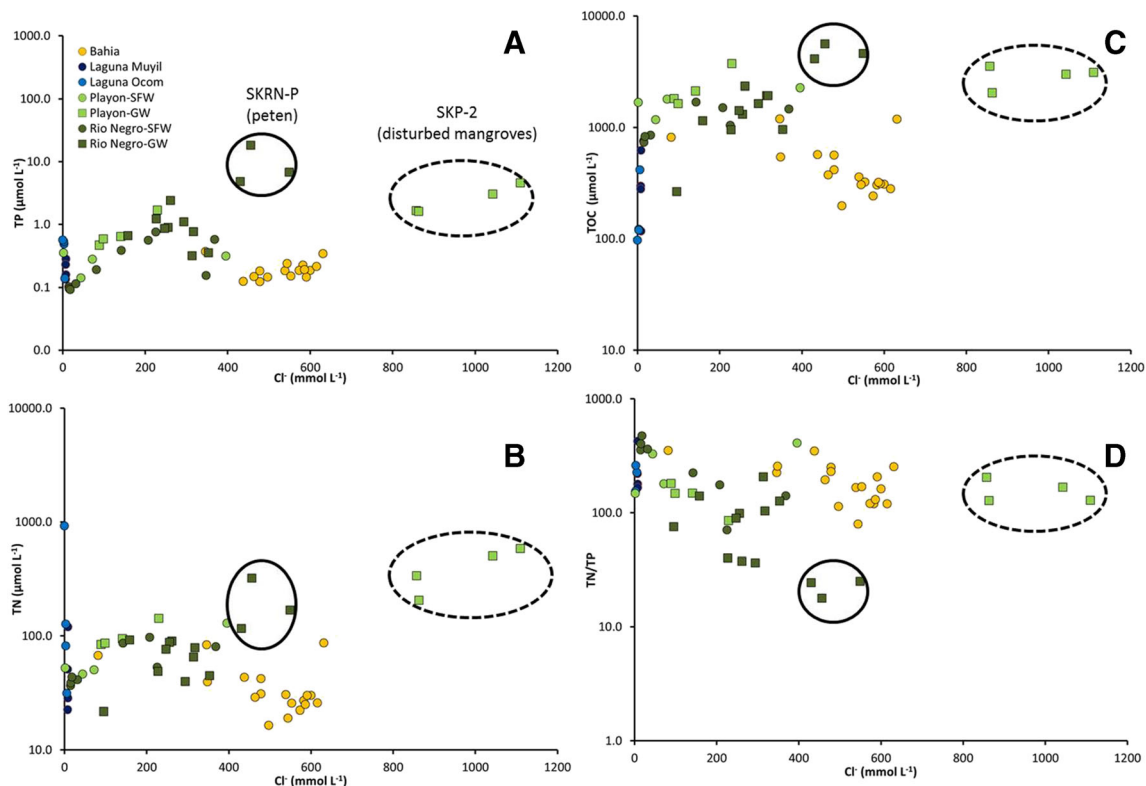


**Fig. 6** Semi-log plots of chloride concentration versus **a** total phosphorus concentrations, **b** total nitrogen, **c** total organic carbon, and **d** TN:TP ratios from all samples collected in the Sian Ka'an Biosphere Reserve.

Outlying samples from sites SKRN-P (peten) and SKP-2 (disturbed mangroves) are circled in black

and Bahia de la Ascension had higher TN/TP ratios than those from May 2012. The average TN/TP ratios were lowest in pore water and groundwater samples collected in Rio Negro and Playon. There was an apparent decrease in TN/TP ratios with increasing  $\text{Cl}^-$  concentrations from  $\sim 15$  to  $250 \text{ mmol L}^{-1}$ , followed by an increase in TN/TP ratio above  $\text{Cl}^-$  concentrations of  $\sim 300 \text{ mmol L}^{-1}$  (Fig. 6d).

The PHREEQC model results indicated that all of the water samples were undersaturated with respect to gypsum and anhydrite, while most samples were at saturation or supersaturated with respect to calcite, aragonite, and dolomite (Table 2). Water samples from Laguna Muyil and Playon tended to be more undersaturated with respect to the evaporite minerals (gypsum and anhydrite) than the water samples from Laguna Ocom and Rio Negro (Table 2). For instance, saturation index values for gypsum and anhydrite were generally less than  $-2.3$  and  $-1.5$  for water samples collected at Laguna Muyil and Playon, respectively. Meanwhile, samples collected from Laguna Ocom and Rio Negro were slightly less undersaturated, with saturation index values greater than  $-2$  at Laguna Ocom and greater than  $-1.5$  at Rio Negro (Table 2). Only two samples collected from Laguna Muyil, Muyil Cenote1, and Laguna Muyil, were slightly undersaturated with respect to the carbonate minerals. Groundwater samples collected at Playon in December 2010 were both undersaturated or near equilibrium with respect to aragonite and calcite (Table 2). The  $\log p\text{CO}_2$  of surface water in the Bahia de la Ascension was close to current atmospheric concentrations ranging between  $-3.84$  and  $-3.01$  with a mean of  $-3.66$ . Pore water and groundwater samples had the highest  $\log p\text{CO}_2$  values ranging between  $-2.67$  and  $-0.72$  (Table 2). Fresh groundwater had moderate  $\log p\text{CO}_2$  values ranging between  $-3.07$  and  $-1.71$ .

#### Water Sources and Principal Component Analysis

Various water sources were identified from the chemical constituents. Plots of  $\text{Cl}^-$  and  $\text{SO}_4^{2-}$  concentrations provided evidence of two distinct inland fresh water sources and a seawater end-member (Fig. 7a). Similarly,  $\text{SO}_4^{2-}:\text{Cl}^-$  and  $\text{Ca}^{2+}:\text{Na}^+$  ratios separated the water samples into the same end-members (Fig. 7b). Water samples collected around Laguna Ocom and Laguna Muyil separated out as the two freshwater end-members (Fig. 7). Laguna Muyil had  $\text{Cl}^-$  concentrations between  $7.8$  and  $8.41 \text{ mmol L}^{-1}$  and  $\text{SO}_4^{2-}$  concentrations between  $0.4$  and  $0.43 \text{ mmol L}^{-1}$ , while Laguna Ocom ranged between  $0.3$  and  $6.0 \text{ mmol L}^{-1}$  and  $2.2$ – $4.2 \text{ mmol L}^{-1}$ , for  $\text{Cl}^-$  and  $\text{SO}_4^{2-}$ , respectively (Table 1; Fig. 7). The water from the St. Isabel well at Laguna Ocom had the lowest ionic concentrations and tended to plot by itself (Figs. 3 and 7). Laguna Ocom also had higher  $\text{SO}_4^{2-}:\text{Cl}^-$  ratios relative to Laguna Muyil and seawater samples (Fig. 7b). Water samples collected in the Bahia de la Ascension generally had the highest concentrations of ions but

exhibited the lowest ratios of  $\text{SO}_4^{2-}:\text{Cl}^-$  and  $\text{Ca}^{2+}:\text{Na}^+$  (Fig. 7b).

Water samples along the Rio Negro represented a mixture of freshwater from Laguna Ocom and the seawater from the bay. Water samples from Playon on the other hand, represented a mixture of freshwater from the north in Laguna Muyil with seawater in from the bay (Figs. 3 and 7). Surface water samples collected at Playon and Rio Negro in December 2010 generally plotted closer to the freshwater end-members. Sub-surface samples collected at SKP2, in the disturbed mangroves, plotted separately as the ionic concentrations were much higher than those found in seawater and indicated hypersaline ( $>40$  psu) conditions (Figs. 6 and 7).

The PCA utilized seven dissolved constituents (alkalinity,  $\text{Cl}^-$ ,  $\text{SO}_4^{2-}$ ,  $\text{Na}^+$ ,  $\text{K}^+$ ,  $\text{Mg}^{2+}$ , and  $\text{Ca}^{2+}$ ) and resulted in two principal components that comprised 97.3 % of the variability of the water samples, U1 (79.7 %) and U2 (17.6 %) (Table 3). The first component, U1, made up 79.7 % of the variability and was defined by  $\text{Cl}^-$ ,  $\text{SO}_4^{2-}$ ,  $\text{Na}^+$ ,  $\text{K}^+$ ,  $\text{Mg}^{2+}$ , and  $\text{Ca}^{2+}$ . Meanwhile, the second component, U2, was defined by alkalinity and explained 17.6 % of the variability (Table 3). Two end-members identified by the PCA were similar to the end-members defined earlier by the chemical analysis, seawater and freshwater. According to the PCA, there was also a third end-member which was identified as peat groundwater (Fig. 8). Water from the Bahia de la Ascension plotted with the seawater end-member, as identified earlier by the ionic concentrations (Figs. 7 and 8). Laguna Muyil and Laguna Ocom samples clustered close together near the fresh water end-member. The peat groundwater end-member was identified by higher relative alkalinity and  $\text{Ca}^{2+}$  concentrations.

All surface water samples collected at Rio Negro and Playon plotted between a fresh water source and the seawater source, regardless of the time of year (Fig. 8). May 2012 surface water samples tended to plot closer to the seawater end-member and alternatively the December 2010 samples plotted closer to the fresh water end-member. All subsurface samples (e.g., PW-20, PW-50, and GW) plotted above a mixing line connecting fresh water from Laguna Muyil and Laguna Ocom to seawater in the Bahia de la Ascension. These samples have higher relative concentrations of  $\text{Ca}^{2+}$  and alkalinity concentrations. The pore water and groundwater samples from the disturbed mangrove site at Playon (SKP-2) plotted outside and to the right of the three end-members because these samples had much higher ionic concentrations and were considered hypersaline with salinities in excess of 40 (Table 1; Fig. 8).

The second PCA, which involved all the ionic constituents except for alkalinity, exhibited similar patterns as the previous PCA with 97.7 % of the variability being described by two principal components U1 (91.4 %) and U2 (6.2 %). The first two components represent the same chemical constituents as the first PCA analysis, but this time only  $\text{Ca}^{2+}$  comprised U2 (Table 4). The same three end-members were identified,

**Table 2** Summary of saturation indices for gypsum, anhydrite, aragonite, calcite, dolomite, and log  $p\text{CO}_2$  for all water samples collected in the Sian Ka'an Biosphere Reserve

Date	Site	Type	Sample name	Charge balance	Gypsum	Anhydrite	Aragonite	Calcite	Dolomite	$\text{CO}_2$ (g)
Dec-10	Bahia de la Ascension	SFW	SKP-109	4.84E-02	-1.13	-1.33	0.76	0.9	2.74	-3.42
Dec-10		SFW	SKP-111	5.29E-02	-1.14	-1.35	0.89	1.04	3	-3.44
Dec-10		SFW	SKRN-81	1.20E-02	-1.5	-1.72	0.61	0.75	2.03	-3.01
Dec-10		SFW	SKRN-82	2.30E-02	-1.21	-1.41	0.77	0.91	2.65	-3.45
Dec-10	Playon	GW	PA-well	-8.23E-04	-2.45	-2.67	0.3	0.44	0.6	-2.22
Dec-10		SFW	SK-lagoon	5.70E-02	-1.22	-1.43	1.02	1.16	3.18	-3.17
Dec-10		SFW	SKP-1	-5.09E-03	-2.24	-2.45	0.47	0.61	1.59	-2.31
Dec-10		GW	SKP-1	-4.81E-03	-1.76	-1.98	-0.6	-0.46	-0.35	-1
Dec-10		GW	SKP-2	5.03E-02	-0.72	-0.91	-0.06	0.08	1.15	-1.1
Dec-10	Rio Negro	SFW	SKRN-0	3.39E-03	-1.54	-1.75	0.33	0.47	1.09	-2.28
Dec-10		GW	SKRN-1	2.38E-02	-1.02	-1.23	0.19	0.33	1.23	-0.69
Dec-10		SFW	SKRN-1	2.40E-03	-1.54	-1.75	0.45	0.6	1.37	-2.73
Dec-10		SFW	SKRN-2	6.94E-04	-1.6	-1.82	0.58	0.72	1.75	-2.88
Dec-10		SFW	SKRN-20	3.67E-03	-1.6	-1.82	0.69	0.83	1.88	-2.78
May-12	Bahia de la Ascension	SFW	SK-82	6.83E-02	-1.08	-1.28	0.9	1.04	3.03	-3.83
May-12		SFW	SK-109	5.86E-02	-1.12	-1.32	0.73	0.88	2.67	-3.37
May-12		SFW	SK-111	-2.48E-03	-1.08	-1.29	0.91	1.05	3.03	-3.84
May-12		SFW	SK-117	1.41E-01	-1.18	-1.39	0.9	1.04	3.03	-3.84
May-12		SFW	SK-118	3.39E-02	-1.12	-1.32	0.93	1.08	3.08	-3.81
May-12		SFW	SK-124	5.78E-02	-1.12	-1.32	0.93	1.08	3.01	-3.79
May-12		SFW	SK-126	4.09E-02	-1.1	-1.3	0.86	1.01	2.95	-3.57
May-12		SFW	SK-127	1.79E-02	-1.12	-1.32	0.77	0.92	2.76	-3.45
May-12		SFW	SK-128	1.47E-03	-1.08	-1.28	0.75	0.89	2.7	-3.38
May-12		SFW	SK-129	-1.45E-02	-1.07	-1.28	0.83	0.97	2.88	-3.69
May-12	Laguna Muyil	Cenote	Muyil Cenote1	-2.22E-04	-2.47	-2.69	-0.24	-0.1	-0.18	-1.96
May-12		Cenote	Muyil Cenote3	1.42E-03	-2.34	-2.56	0.4	0.54	0.89	-1.71
May-12		Cenote	Laguna Muyil	5.65E-04	-2.72	-2.94	-0.68	-0.53	-0.81	-1.72
May-12	Laguna Ocom	Cenote	Ocum	4.44E-03	-1.7	-1.92	0.69	0.83	1.87	-3.07
May-12		Cenote	St Isabel	1.09E-03	-2.95	-3.17	0.26	0.4	-0.26	-1.94
May-12		Cenote	Sijjil	5.96E-03	-1.28	-1.5	0.21	0.36	0.54	-1.45
May-12		Cenote	Cenote1	5.70E-03	-1.65	-1.87	1.41	1.55	2.91	-2.82
May-12	Rio Negro	20	SKRN-0	2.94E-02	-1.18	-1.39	0.42	0.57	1.63	-1.91
May-12		20	SKRN-P	3.12E-02	-0.68	-0.89	-0.03	0.11	0.76	-0.84
May-12		20	SKRN-1	5.09E-02	-1.15	-1.36	0.01	0.15	0.94	-1.74
May-12		20	SKRN-2	2.38E-02	-1.02	-1.23	0.58	0.72	2.07	-1.81
May-12		50	SKRN-0	2.13E-02	-1	-1.22	0.28	0.42	1.28	-1.17
May-12		50	SKRN-P	3.29E-02	-0.61	-0.81	0.1	0.24	1.01	-0.79
May-12		50	SKRN-1	4.81E-02	-1.13	-1.34	0.07	0.21	1.04	-1.41
May-12		50	SKRN-2	3.19E-02	-1.21	-1.42	0.62	0.76	2.16	-1.27
May-12		GW	SKRN-0	2.08E-02	-1.04	-1.25	0.26	0.4	1.31	-1.26
May-12		GW	SKRN-P	1.17E-02	-0.58	-0.79	0.21	0.36	1.25	-0.72
May-12		GW	SKRN-1	4.18E-02	-1.06	-1.27	0.44	0.59	1.74	-1.04
May-12		GW	SKRN-2	1.78E-02	-1.19	-1.41	0.22	0.37	0.96	-1.16
May-12		SFW	SKRN-0	2.59E-02	-1.16	-1.38	0.71	0.85	2.2	-2.81
May-12		SFW	SKRN-P	2.19E-02	-1.16	-1.37	0.78	0.92	2.45	-3.05
May-12		SFW	SKRN-1	1.01E-01	-1.28	-1.5	0.78	0.92	2.52	-3.1
May-12		SFW	SKRN-2	3.00E-02	-1.07	-1.28	1.01	1.15	3.02	-3.51
May-12	Playon	SFW	SKP-1	-6.65E-06	-1.79	-2.01	0.68	0.82	2.01	-2.67

**Table 2** (continued)

Date	Site	Type	Sample name	Charge balance	Gypsum	Anhydrite	Aragonite	Calcite	Dolomite	CO <sub>2</sub> (g)
May-12		20	SKP-1	4.36E-03	-1.7	-1.92	0.26	0.4	1.23	-2.11
May-12		50	SKP-1	3.68E-02	-1.35	-1.56	0.47	0.61	1.87	-1.77
May-12		GW	SKP-1	3.84E-03	-1.53	-1.74	0.4	0.55	1.65	-2.24
May-12		SFW	SKP-2	6.65E-01	a	a	1.15	1.29	3.42	-3.69
May-12		20	SKP-2	1.04E+00	a	a	0.22	0.37	1.62	-1.9
May-12		50	SKP-2	1.31E+00	a	a	0.32	0.47	1.89	-1.59
May-12		GW	SKP-2	1.21E+00	a	a	0.48	0.63	2.14	-1.86

a Missing data from samples

seawater, fresh groundwater, and peat groundwater; however, there was a more apparent peat groundwater end-member characterized by groundwater samples collected from SKRN-P (peten) (Fig. 9).

The surface water samples in the second PCA from Rio Negro and Playon, once again, plotted between the fresh

groundwater and seawater end-members. These samples also exhibited mixing associated with the peat groundwater end-member (Fig. 9). Water samples collected from the SKP-1 tended to plot closer to the freshwater end-member. Meanwhile, samples from Rio Negro plotted in the center of all three end-members. A seasonal signal was also observed in the surface water at Rio Negro whereby samples collected in December 2010 plotted closer to the fresh groundwater end-member and the May 2012 samples tended to plot as a mix of all three end-members (Fig. 9).

Contributions from each end-member were determined for all of the water samples using the PCA without alkalinity (Fig. 10). Samples plotting closer to the end-members had higher contributions from that particular end-member. Water samples from the Bahia de la Ascension generally contained greater than 80 % of seawater with the remaining fraction composed of freshwater (Fig. 10). Sampling locations near the mouth of Rio Negro (e.g., SK-81, SK-82) exhibited the greatest fluctuation between sampling periods in the amount of freshwater contained in the samples (Fig. 10). Surface water samples at Rio Negro from December 2010 had freshwater end-member contributions ranging between 35 % at the mouth (SK-82) to over 95 % in the upper reaches of the river (SKRN-0) (Fig. 10). Fresh water contributed between ~60 and 90 % at SKP-1, but had little to no contribution at SKP-2 (Fig. 10). Surface water samples collected from Rio Negro in December 2010 contained little contribution from peat groundwater while the May 2012 samples were composed of 10–20 % peat groundwater (Fig. 10). There was little contribution of peat groundwater to samples from Playon, regardless of the collection date. The peten site in Rio Negro (SKRN-P) had the highest contribution of peat groundwater, comprising 80–100 % of the samples.

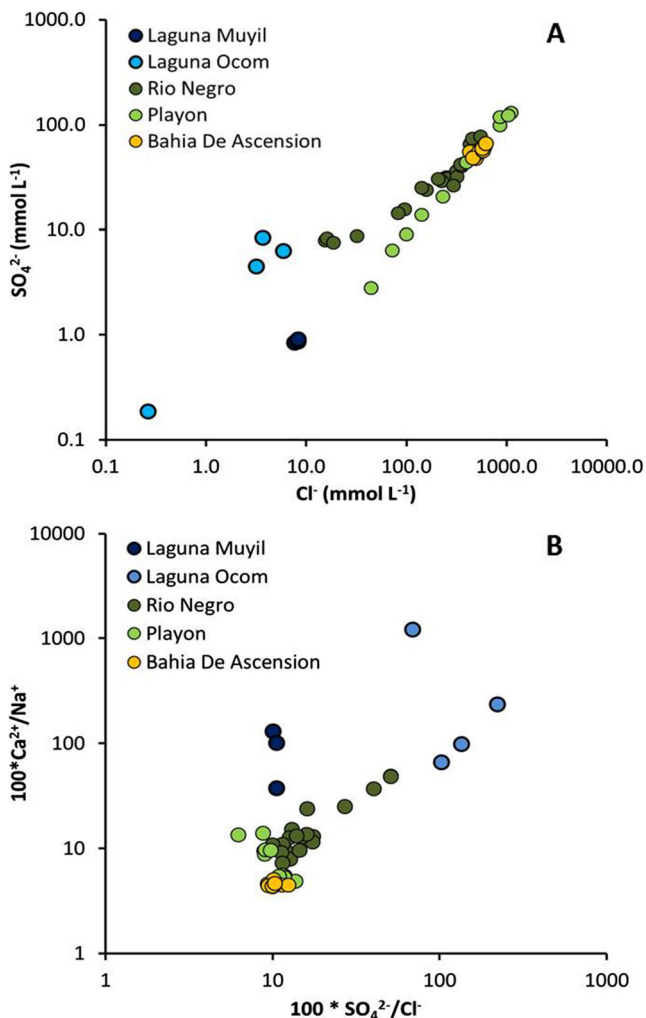


**Fig. 7** Log-log plots of **a** chloride (Cl<sup>-</sup>) versus sulfate (SO<sub>4</sub><sup>2-</sup>) concentrations and **b** Cl<sup>-</sup>/SO<sub>4</sub><sup>2-</sup> versus calcium/sodium ratios for all water samples collected in the Sian Ka'an Biosphere Reserve

## Discussion

### End-Member Mixing

Two distinct fresh water sources were identified from the water samples collected from in and around Sian Ka'an and

**Table 3** Results of two principal component analysis (with alkalinity) shown as factor loadings for all principal components with the percent variability associated with each principal component

Parameter	Principal components						
	U1	U2	U3	U4	U5	U6	U7
Alkalinity	0.16	0.97	-0.16	0.01	0.00	0.00	0.00
Cl <sup>-</sup>	0.99	-0.12	-0.06	0.03	-0.04	0.07	-0.01
SO <sub>4</sub> <sup>2-</sup>	0.99	-0.01	0.06	0.15	-0.03	-0.04	0.01
Na <sup>+</sup>	0.99	-0.14	-0.06	-0.04	0.05	0.01	0.02
K <sup>+</sup>	0.96	-0.21	-0.11	-0.11	-0.05	-0.04	0.00
Mg <sup>2+</sup>	0.99	-0.07	-0.04	0.03	0.07	-0.01	-0.02
Ca <sup>2+</sup>	0.85	0.45	0.27	-0.07	0.00	0.01	0.00
Variability (%)	79.74	17.57	1.76	0.62	0.18	0.12	0.01
Cumulative %	79.74	97.31	99.07	99.69	99.87	99.99	100.00

strongly suggest a groundwater hydraulic divide between the two regions, Laguna Ocom and Laguna Muyil. The water collected in the cenotes near Laguna Ocom contained elevated concentrations of SO<sub>4</sub><sup>2-</sup> and exhibited higher SO<sub>4</sub><sup>2-</sup>:Cl<sup>-</sup> ratios when compared to the cenotes of Laguna Muyil (Fig. 7). An areally extensive impact breccia containing limestones, silicates, and evaporite sequences has been identified in the central and southeastern portion of the state of Quintana Roo as a result of the Chicxulub impact (Perry et al. 2003; Leticariu et al. 2006). The evaporite material is primarily composed of the sulfate-rich minerals anhydrite (CaSO<sub>4</sub>) and gypsum (CaSO<sub>4</sub>·2H<sub>2</sub>O), both of which have higher solubility than calcite or aragonite. Water samples collected from groundwater wells, cenotes, and lakes in surrounding sites to the west and to the south, in a region known to contain an evaporite sequence, have been shown to contain elevated SO<sub>4</sub><sup>2-</sup> concentrations relative to water samples collected in more northern areas of the peninsula (Perry et al. 1995, 2002).

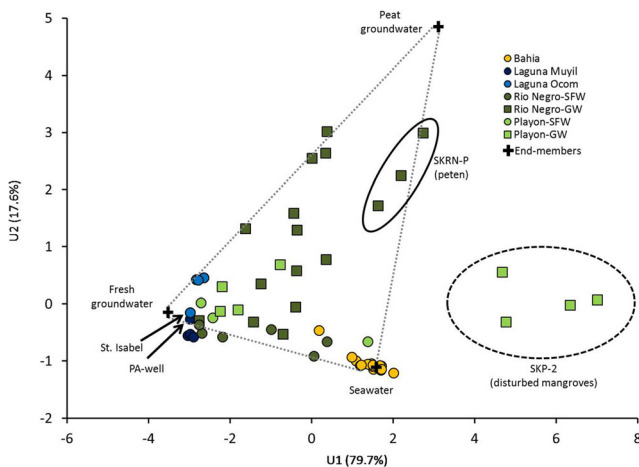


**Fig. 8** Principal component plot (with alkalinity) for water chemistry data from the Sian Ka'an Biosphere Reserve plotted in *U* space as defined by the *orthogonal projections* from the principal component analysis. Recognized end-members are shown: fresh groundwater, seawater, and peat groundwater. Outlying samples from SKP-2 (disturbed mangroves) are circled in black

The boundary and depth of the evaporite sequence has not yet been fully constrained because of the poor consolidation of the geologic material that has led some studies to recognize various areas as impact ejecta (Pope et al. 2005) or Holocene alluvium (Salinas-Prieto et al. 2007). More recent studies using microscopic analyses and Sr<sup>2+</sup> isotopic data have further constrained this region and identified locally breached perched water tables from dissolution evaporates and Albion Formation (Perry et al. 2002). The cenotes around Laguna Ocom are most likely hydrologically connected to the sulfate-rich evaporite layers. The persistent undersaturation with respect to gypsum and anhydrite of all of the water samples collected in this study is similar to other studies in the region (Perry et al. 2002) (Table 2) and indicates that the groundwater in the region has not been able to equilibrate with those minerals.

The water chemistry from Laguna Muyil is characterized as a calcium-bicarbonate type water with little to no sulfate which is indicative of water in contact with limestone. Saturation indices calculated using PHREEQC indicate that all of the water samples collected during this study were saturated or near-saturated with respect to calcite and aragonite except for

**Table 4** Results of principal component analysis (without alkalinity) shown as factor loadings for all principal components with the percent variability associated with each principal component

Parameter	Principal components					
	U1	U2	U3	U4	U5	U6
Cl <sup>-</sup>	0.99	-0.12	-0.02	-0.07	0.07	-0.01
SO <sub>4</sub> <sup>2-</sup>	0.95	0.13	0.28	0.01	-0.01	0.00
Na <sup>+</sup>	0.99	-0.15	-0.04	-0.01	-0.02	0.03
K <sup>+</sup>	0.96	-0.23	-0.05	0.13	0.01	-0.01
Mg <sup>2+</sup>	0.99	-0.08	-0.06	-0.07	-0.06	-0.02
Ca <sup>2+</sup>	0.85	0.51	-0.12	0.02	0.01	0.00
Variability (%)	91.44	6.25	1.70	0.45	0.14	0.02
Cumulative %	91.44	97.69	99.39	99.84	99.98	100.00

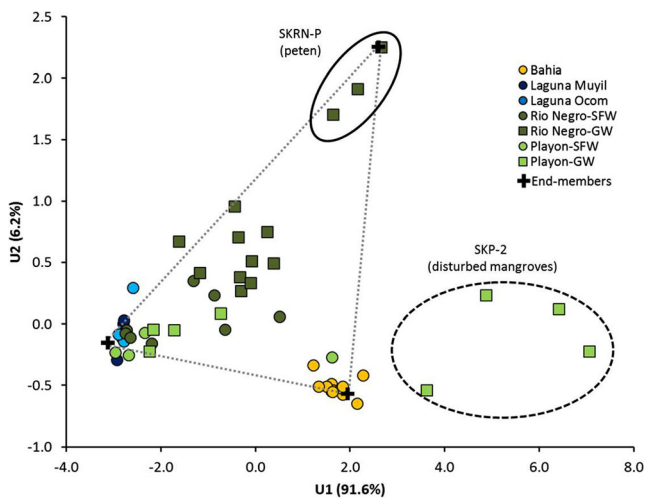


**Fig. 9** Principal component plot (without alkalinity) for water chemistry data from the Sian Ka'an Biosphere Reserve plotted in *U* space as defined by the *orthogonal projections* from the principal component analysis. Recognized end-members are shown: fresh groundwater, seawater, and peat groundwater. Outlying samples from SKP-2 (disturbed mangroves) are circled in black

two samples at Laguna Muyil that were slightly undersaturated (Table 2). The inland waters of Laguna Muyil may be more representative of recharge water that has not had time to reach equilibrium with respect to the carbonate minerals calcite and aragonite.

The differentiation in water chemistry between the two fresh water sources, Laguna Muyil and Laguna Ocom, suggest a hydraulic divide between the two regions (Figs. 3 and 7). Groundwater flows in the Yucatan have been mapped by a number of researchers and are reviewed in Bauer-Gottwein et al. (2011). The ionic water chemistry data indicates a clear connection between surface water along Rio Negro and freshwater around Laguna Ocom and is consistent with an eastward groundwater flow that has been mapped in the region west of Laguna Ocom (Bauer-Gottwein et al. 2011). The groundwater flow paths of the Yucatan are reviewed by Bauer-Gottwein et al. (2011), where multiple groundwater pathways have been mapped from the central peninsula to the coast as well as northwestward from northern Belize to Tulum. Water chemistry between Laguna Muyil and Laguna Ocom measured in the present study does not indicate any mixing between the two freshwater end-members. Therefore, the northwestward groundwater pathway previously measured may be part of another hydrogeologic section that is not in contact with evaporite sequences in the Albion formation as suggested by Perry et al. (2009) and could flow through northeast-southwest trending fractures and faults suggested by Gondwe et al. (2010).

Oxygen isotopic values,  $\delta^{18}\text{O}$ , from the freshwater cenotes Laguna Ocom and Laguna Muyil ( $-5.17\text{‰} > \delta^{18}\text{O} > -1.78\text{‰}$ ) are very similar to  $\delta^{18}\text{O}$  values of rainfall measured in the Yucatan at Merida ( $-1.5\text{‰}$ ; Perry et al. 2003) and Celestun [ $-2.9\text{‰}$ ; Stalker et al. (accepted in Estuaries and Coasts)]; and

in nearby Veracruz and San Salvador ( $-4.0$  and  $-6.5\text{‰}$ , respectively; Lachniet and Patterson 2009) and south Florida ( $-3.6\text{‰} > \delta^{18}\text{O} > -2.8\text{‰}$ ; Price et al. 2006). The freshwater in the cenotes is expected to flow through the groundwater system and discharge to the surface water upstream of SKRN-O and SKP-1 at Rio Negro and Playon, respectively. Once the fresh groundwater discharges to the surface, it undergoes evaporation and mixes with water from the Bahia de la Ascension, thereby increasing the isotopic ratios of  $\delta^{18}\text{O}$  and  $\delta^2\text{H}$  along the evaporation and seawater mixing lines (Fig. 4). Heavier  $\delta^{18}\text{O}$  and  $\delta^2\text{H}$  values were measured in the upstream reaches of Rio Negro (SKRN-0) relative to the mouth (SKRN-2) possibly suggesting longer transit times in the upper reaches of the river. Freshwater may also discharge

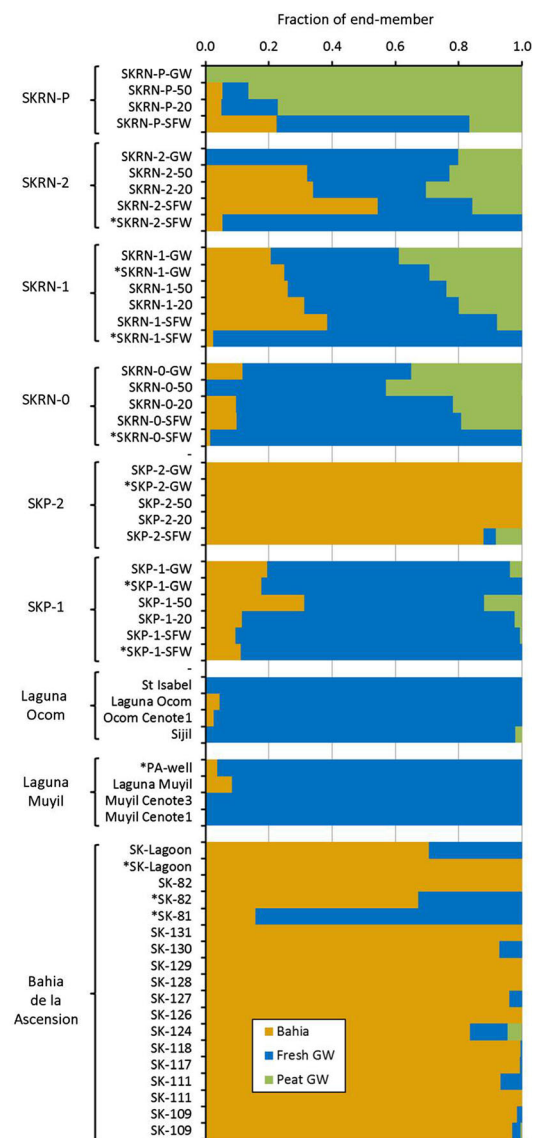


**Fig. 10** Percentage of each end-member contributions, fresh groundwater, seawater, and peat groundwater, calculated for each water sample using the end-member mixing model

at other localities along Rio Negro, as suggested by the greater freshwater contribution in the groundwater at SKRN-2 (Fig. 10). Lateral discharge from the river banks could also contribute to the surface water (Santos et al. 2010) though the results indicate very little contribution of peat groundwater to the surface water in other locations besides SKRN-P (Fig. 10).

### Nutrient Dynamics

The estuarine zone of the SKBR can be characterized as an oligotrophic-mesotrophic system as a result of the low nutrient concentrations in the surface water similar to other environments in the Yucatan (Chelum lagoon; Herrera-Silveira et al. 2002), Belize (Rejmánková and Komárková 2000) and south Florida (Childers et al. 2006). The relatively low TP concentrations and high TN:TP ratios measured in this study suggest that the SKBR is a phosphorus-limited system, typical of other carbonate-rich environments (Short et al. 1990; Fourqurean et al. 1992; Jensen et al. 1998; Rejmánková and Komárková 2000). Surface water TN and TP concentrations at Rio Negro and Playon were very similar to the concentrations measured in the surface waters of the southeastern Everglades, where concentrations range between  $\sim 25$  and  $100 \mu\text{mol L}^{-1}$  for TN and  $\sim 0.2$  and  $1.5 \mu\text{mol L}^{-1}$  for TP (Childers et al. 2006). Total phosphorus concentrations in the coastal SKBR exhibit analogous spatial variability as the “upside down” nature of the Florida Coastal Everglades in which the limiting nutrient (i.e., TP) supply originates from a marine source (Childers et al. 2006). The lower nutrient concentrations in the surface water of Rio Negro and Playon and the Bahia de la Ascension suggest that nitrogen and phosphorus may be removed from the water column quickly via biological processes, phosphorus adsorption to carbonate sediments, or redox processes (Short et al. 1990).

The oligotrophic-mesotrophic nature of SKBR differs from mesotrophic-eutrophic lagoonal estuaries found along the northwestern coast (Celestun and Dzilam lagoons; Herrera-Silveira et al. 2002), northern coast (Ria Largatos; Valdes and Real 2004) and eastern coast of the Yucatan (Mutchler et al. 2007). Long surface water residence times and anthropogenic activity have been shown to contribute to the higher nutrient concentrations in the coastal lagoons (Medina-Gómez and Herrera-Silveira 2003; Herrera-Silveira et al. 2004). However, the SKBR and vicinity are more segregated from the anthropogenic pressures from the northwest and northeast Yucatan and the surface waters in the SKBR exhibited phosphorus-limited conditions during both sampling periods.

Groundwater and pore water samples had elevated nutrient concentrations relative to the overriding surface water. Among the groundwater and pore water, the samples collected from the SKP-2 had TP concentrations an order of magnitude higher than the other samples, save a groundwater sample at SKRN-P and SKP-1 (Fig. 5). The elevated TP concentrations

may have been a result of the release of phosphorus from the dissolution of calcium carbonate. In that respect, there would be an accompanied increase in calcium concentrations above what would be conserved by mixing with seawater which was not observed. Calcium concentrations measured at SKP-2 plotted slightly above the freshwater-seawater conservative mixing line (Fig. 11). The lack of mangrove vegetation at SKP-2 and the hypersaline condition suggests that a heterotrophic environment exceeds that of autotrophy which increases the oxidation of organic matter, and in turn dissolves calcium carbonate (Fourqurean et al. 2012). The dissolution of calcium carbonate might not be as strong as that from SKRN-P, because  $\text{Ca}^{2+}$  concentrations measured in the subsurface as SKP-2 plot above, but closer, to the freshwater-seawater conservative mixing line (Fig. 11). Salinities greater than 9 have been shown to have a propensity to release more Ca-bound phosphorus in carbonate-rich sediments in Florida Bay (Zhang and Huang 2011). Alternatively, the high TP concentration in the groundwater at SKRN-P was associated with elevated  $\text{Ca}^{2+}$  concentrations with respect to the freshwater-seawater conservative mixing line and may suggest that there is groundwater discharge to the surface water around the peten at SKRN-P (Figs. 6 and 11). The highest TP concentrations measured in the surface water during the dry season were obtained near SKRN-P and SKRN-1 and could be sourced by the possible coastal groundwater discharge around the nearby peten, as many petens are known to contain groundwater springs (Adame et al. 2013). Lastly, the PCA without alkalinity indicated that the surface water collected at Rio Negro in May 2012 contained 10–20 % of peat groundwater (Fig. 10).

The petens are the most productive coastal vegetation in the Yucatan (Adame et al. 2013). This high productivity is fueled

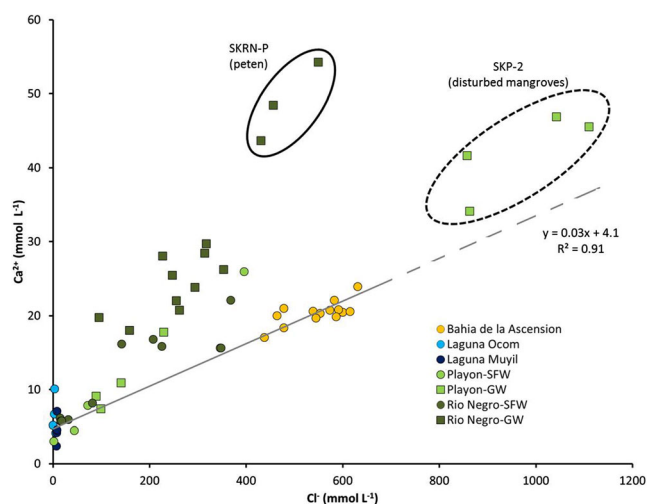


**Fig. 11** Chloride and calcium concentrations from water samples collected in the Sian Ka'an Biosphere Reserve. A conservative freshwater-seawater mixing line is plotted as a black line. Samples above the line indicate excess calcium

by a combination of factors. First, freshwater spring inputs with higher nutrient concentrations, mainly N-favored high productivity, are associated with petens. Secondly, the relative isolation of these vegetation types make them efficient in the nutrient recycling, and thirdly, petens are biodiversity hotspots where fauna could allow for the import nutrients, mainly phosphorus (Adame et al. 2013). In addition, several biogeochemical process could lead to increased phosphorus concentrations that were measured in the peten, from the release of phosphorus from marine sediments found at the base of the groundwater well or from the breakdown of organic matter.

#### Groundwater/Surface Water Disconnect in Disturbed Mangrove Zone

The water from the two sites at Playon exhibit two distinct chemical signatures despite being only a few meters apart. The site north of the road, SKP-1 is derived primarily from a freshwater source similar to the water at Laguna Muyil while SKP-2 is characterized as evaporated seawater with little to no contribution of freshwater (Figs. 9 and 10). The primary reason for the chemical dichotomy between these two nearby sites is the hydraulic barrier created by the slightly elevated (~1 m above the marsh surface) dirt road separating the two sites. The road essentially cuts off surface water runoff from the north causing it to be dammed north of the dirt road. The higher freshwater head levels north of the road allow for more infiltration of the surface water into the subsurface sediments. The low peat groundwater signal (<20 %) that is characterized by elevated  $\text{Ca}^{2+}$  and alkalinity may also suggest faster infiltration and lower residence times, inhibiting the decomposition of organic matter that leads to increased alkalinity. A small culvert in the road does not allow for sufficient water exchange between the north and south side of the road. The isotopic and ionic chemistry from the water at SKP-2 suggests that seawater from the Bahia de la Ascension entered the area through tidal propagation and then evaporated within the basin causing hypersaline conditions. Mangroves on the north side of the road at Playon were observed to be in more productive and healthier conditions than the hypersaline environment to the south. The different chemical signatures between both sides of the road at Playon could be useful as mangrove function indicator for monitoring and restoration programs.

#### Groundwater Chemistry and Groundwater Discharge

Elevated concentrations of  $\text{Ca}^{2+}$  have been used as an indicator for brackish groundwater discharge (Price et al. 2006). Concentrations of  $\text{Ca}^{2+}$  above what are expected from conservative mixing of freshwater and seawater were observed in the surface water samples at Rio Negro (Fig. 11). This additional source of  $\text{Ca}^{2+}$  most likely comes from the dissolution of the

limestone bedrock and carbonate sediments at the interface between fresh groundwater and intruding seawater as seen in other regions of the Yucatan (Back et al. 1986), the Bahamas (Smart et al. 1988) and in south Florida (Price et al. 2006). The brackish groundwater mixing zone can become undersaturated with respect to calcite and aragonite even though both end-members may be saturated (Wigley and Plummer 1976; Sanford and Konikow 1989; Rezaei et al. 2005). Only a few subsurface samples were collected in Rio Negro and Playon that exhibited undersaturation with respect to calcite and aragonite, while many of the subsurface samples were at or just above S.I. values (Table 2).

Petens studied in the SKBR were found to have the highest carbon stocks and were associated with freshwater springs (Adame et al. 2013). The pore water and groundwater collected in the peten located at SKRN-P had little contribution from the fresh groundwater end-member (<18 %) or from seawater (<8 %) (Fig. 10). This small contribution of fresh groundwater and seawater at SKRN-P was in contrast to groundwater collected at the other three groundwater sites along Rio Negro that contained a 30–60 % fresh groundwater signal (Fig. 10). The alkalinity in the subsurface peten samples were similar to other subsurface samples collected in Rio Negro and Playon (Table 1), as well as other similar sites in the Florida Everglades (Zapata-Rios and Price 2012), Australia (Maher et al. 2013), and the Dominican Republic (Sherman et al. 1998). Despite the similarities in alkalinity, the peten samples were distinctly different than the other samples in Rio Negro because of the elevated  $\text{Ca}^{2+}$  concentrations (Table 1; Figs. 9 and 10). The higher  $\text{Ca}^{2+}$  concentrations at SKRN-P suggest there may be slightly more dissolution of calcite and aragonite as a result of higher  $\log p\text{CO}_2$  and corresponding lower pH values associated with the breakdown of organic matter and mangrove root respiration in the subsurface (Bouillon et al. 2008).

The complex karst geology and the preferential flow through the below-ground cave network and faults and fractures may control the location and extent of the coastal groundwater discharge zone. Groundwater at the upstream stream site in Rio Negro, SKRN-0, contained approximately 20 % seawater while SKRN-1 and SKRN-2 showed no signs of seawater. One suggestion of this relationship could be coastal groundwater discharge from two different aquifer sources. A perched and regional aquifer have been identified in areas inland of Rio Negro (Perry et al. 2009) with more dynamic groundwater level changes and higher pressure heads in the perched aquifer (Gondwe et al. 2010). Coastal groundwater discharge in the peten could be sourced from a deeper aquifer than may have been breached by the aquitard; separating the two aquifers either by dissolution or from fracturing and faulting (Gondwe, et al. 2010) while the perched aquifer containing fresher water may be able to reach the coast. Perry et al. (2011) has also suggested that groundwater from the Rio Hondo region, south of the SKBR, could

flow northwards through the Rio Hondo fault zone and discharge into the southern end of the Bahía de la Ascension. The lack of research and understanding of the coastal geology in the SKBR make these results difficult to interpret and further hydrogeochemical and resistivity studies are needed to constrain the local geology.

Water samples collected in the subsurface also contained higher alkalinity relative to the surface water (Table 1). These elevated concentrations have been measured in the pore water and groundwater of similar mangrove environments and are a result of sulfate reduction (Ovalle et al. 1990), carbonate dissolution (Middelburg et al. 1996) or the addition of CO<sub>2</sub> through autotrophic and heterotrophic respiration (Bouillon et al. 2008). Zapata-Rios and Price (2012) and Lagomasino et al. (submitted to Remote Sensing of Environment) measured high alkalinity and TP in the groundwater and pore water of a dwarf mangrove ecosystem in southwestern Everglades. In addition, brackish groundwater discharge was recorded during the late dry season in the southwestern Everglades (Zapata-Rios and Price 2012). The higher alkalinity measured in the pore water and groundwater sites at Rio Negro, in conjunction with the elevated Ca<sup>2+</sup> and TP concentrations measured in the surface water and groundwater at Rio Negro strongly suggest that coastal groundwater discharge occurs (Price et al. 2006) ~5 km inland around SKRN-P, despite the fact that the surface water alkalinity was an order of magnitude less than the groundwater (Table 1). This groundwater discharge could be associated with seepage from the peat into the surface water from tidal pumping (Maher et al. 2013) or from deeper brackish groundwater discharge associated with the mixing zone between freshwater and seawater intrusion (Price et al. 2006). The combination of groundwater discharge and the discrepancy between alkalinity values between the groundwater and surface water could represent an important dissolved inorganic carbon pathway in Sian Ka'an, and other similar mangrove wetlands like the southern Everglades.

The differences in alkalinity between the groundwater and surface water are also mirrored in the log *p*CO<sub>2</sub> values of the two water types (Table 2). In the surface water, log *p*CO<sub>2</sub> was comparable to current atmospheric conditions (−3.8), whereas groundwater samples in the peat and cenotes tended to be 1–2 orders of magnitude higher suggesting increases of CO<sub>2</sub> from autotrophic and heterotrophic respiration (Bouillon et al. 2008). The PCA that included alkalinity suggested that there was little to no interaction between the groundwater and surface water, which was in contrast to the Ca<sup>2+</sup> and TP concentrations indicating a connection between the two waters. By including alkalinity in the PCA, a clear signal of peat groundwater mixing with surface water at Rio Negro was observed (Figs. 9 and 10). This discrepancy of the loss of alkalinity between the groundwater and surface water was most likely caused by the evasion (outgassing) of CO<sub>2</sub> as the

groundwater discharges to the surface water, which can reach equilibrium in a matter of minutes (Moran 2010). When the high alkalinity, low pH groundwater discharges to the surface water, the CO<sub>2</sub> gas quickly escapes from the surface water to the atmosphere. Moran (2010) showed that when the influent CO<sub>2</sub> concentrations were high (>25 mg L<sup>−1</sup>), the amount of CO<sub>2</sub> degassed from the system varied with salinity where 75 % of CO<sub>2</sub> was degassed for seawater and 87 % for freshwater. This exchange and release of carbon could be substantial because 10–20 % of the surface water at Rio Negro is composed of the peat groundwater end-member (Fig. 10). In their review, Bouillon et al. (2008) discusses the “missing” carbon in mangrove forests and hypothesizes inorganic carbon through CO<sub>2</sub> degassing could help to close the carbon budget. More recently, Maher et al. (2013) suggested that groundwater advection through tidal pumping exported 93–99 % of dissolved inorganic carbon and were an order of magnitude greater than organic carbon exports.

## Conclusions

Using natural geochemistry and chemical tracers in the groundwater and surface water, we were able to discern two distinct upland fresh groundwater sources that eventually discharge into the SKBR; a sulfate-rich groundwater around Laguna Ocom and a calcium-rich groundwater at Laguna Muyil. Water from Laguna Ocom, which is in a primarily rural and agricultural area, feeds water to Rio Negro. Meanwhile, water from Laguna Muyil feeds water to Playon. Water passing through Laguna Ocom, which is in a primarily rural and agricultural area, discharges into Rio Negro. Meanwhile, water at Playon is fed by groundwater from Laguna Muyil, which is located in a more urbanized region. Fresh groundwater from Laguna Ocom was found to be rich in sulfate and most likely caused by dissolution of the calcium-sulfate minerals anhydrite and gypsum which are common to an evaporite layer in the regional subsurface. Fresh groundwater from Laguna Muyil exhibited a calcium carbonate-type chemical signature typical for water-rock interactions with limestones.

Three major sources of water were identified as to contributing to the coastal region of SKBR: fresh groundwater, peat groundwater, and seawater. The peat groundwater end-member was observed in pore water and groundwater samples at Rio Negro and Playon, but with affinity to the downstream sites at Rio Negro (SKRN-P, SKRN-1, SKRN-2). The occurrence of a dirt road at Playon was found to inhibit the exchange of freshwater from the north with seawater from the south. As a result, hypersaline conditions exist south of the road leading to an absence in mangroves and a buildup of nutrients in the subsurface peats. Nutrient and chemical analyses indicate that the SKBR is an oligotrophic-mesotrophic

environment with phosphorus limitations, but were less P-limited in the surface water brackish zone between 200 and 350 mmol L<sup>-1</sup> of Cl<sup>-</sup>, similar to the southeastern Everglades. The highest nutrient concentrations were found in the pore water and groundwater, and more specifically, in the disturbed mangrove site, SKP-2, and the peten site, SKRN-P. Phosphorus concentrations were highest in the mid-estuary and associated with groundwater discharge from petens. The coastal groundwater discharge to the estuarine surface water suggests an autochthonous nutrient source rather than typical allochthonous nutrient sources from upland runoff or marine deposits.

The combination of high alkalinity and high nutrient content in the subsurface discharging to the low alkalinity, low nutrient surface water at Rio Negro demonstrates the importance of this process in water and inorganic carbon exchange. Identifying individual water sources and their mixtures are important in understanding the fate and transport of groundwater as it passes through the ecosystem. Recent trends in tourism development and urbanization encroaching on the northern boundary of the SKBR could push the reserve into more mesotrophic to eutrophic conditions in the near future. The anthropogenic activities in the north and south could change the trophic conditions to the Bahia de la Ascension because each of these developing regions has been identified in the present research to discharge into the bay. The type of human activity in these regions could impact the SKBR in different ways. From the north, tourism development could be more important, but, in the south the agriculture in the region could show more influence. These development practices could make the Bahia del la Ascension strongly vulnerable to eutrophication from two different types of nutrient contamination sources.

The results from the present study have linked previously unknown inland and coastal water sources in the absence of surface water flow. In addition, important nutrient and carbon source pathways were reported via coastal groundwater discharge which could play a role in other oligotrophic, coastal carbonate wetlands like those found elsewhere in the Yucatan and in the Everglades. Changes to the groundwater hydrology caused by natural events and/or exacerbated by increased development, water demands, or waste-water disposal could result in changes to the water chemistry and ecology and put pressure on the coastal wetlands of the SKBR as well as its offshore shallow coastal communities, seagrasses, and coral reefs.

**Acknowledgments** This research was supported directly by the National Science Foundation through the Florida Coastal Everglades Long-Term Ecological Research program under Grant No. DBI-0620409 and the NASA WaterSCAPES program under Grant No. NNX-10AQ13A. Field and travel support were provided by the Comisión Nacional de Áreas Naturales Protegidas (CONANP) and Amigos de Sian Ka'an in Cancun, Mexico; and the Centro de Investigacion y de Estudios Avanzados

(CINVESTAV) Unidad Merida in Merida, Mexico. Additional financial support was provided by the Florida Education Fund McKnight Dissertation Year Fellowship. This is contribution number 690 from the Southeast Environmental Research Center at Florida International University.

## References

- Abesser, C., R. Robinson, and C. Soulsby. 2006. Iron and manganese cycling in the storm runoff of a Scottish upland catchment. *Journal of Hydrology* 326: 59–78. doi:10.1016/j.jhydrol.2005.10.034.
- Adame, M.F., J.B. Kauffman, I. Medina, J.N. Gamboa, O. Torres, J.P. Caamal, M. Reza, and J. Herrera-Silveira. 2013. Carbon stocks of tropical coastal wetlands within the karstic landscape of the Mexican Caribbean. *PLoS One* 8: e56569.
- Back, W., B.B. Hanshaw, J.S. Herman, and J.N. Van Driel. 1986. Differential dissolution of a pleistocene reef in the ground-water mixing zone of coastal Yucatan, Mexico. *Geology* 14: 137–140. doi:10.1130/0091-7613(1986)14<137:DDOAPR>2.0.CO;2.
- Baker, M.A., and P. Vervier. 2004. Hydrological variability, organic matter supply and denitrification in the Garonne river ecosystem. *Freshwater Biology* 49: 181–190. doi:10.1046/j.1365-2426.2003.01175.x.
- Bauer-Gottwein, P., B.N. Gondwe, G. Charvet, L. Maran, M. Rebolledo-Vieyra, and G. Merediz-Alonso. 2011. Review: the Yucatan Peninsula karst aquifer, Mexico. *Hydrogeology Journal*. 19: 507–524. doi:10.1007/s10040-010-0699-5.
- Beddows, P.A. 2004. *Groundwater hydrology of a coastal conduit carbonate aquifer: Caribbean Coast of the Yucatan Peninsula, Mexico*. Evanston, IL: Northwestern University.
- Beddows, P.A., P.L. Smart, F.F. Whitaker, and S.L. Smith. 2007. Decoupled fresh–saline groundwater circulation of a coastal carbonate aquifer: spatial patterns of temperature and specific electrical conductivity. *Journal of Hydrology* 346: 18–32. doi:10.1016/j.jhydrol.2007.08.013.
- Bouillon, S., A.V. Borges, E. Castañeda Moya, K. Diele, T. Dittmar, N.C. Duke, E. Kristensen, S.Y. Lee, C. Marchand, J.J. Middelburg, V.H. Rivera-Monroy, T.J. Smith III, R.R. Twilley. 2008. Mangrove production and carbon sinks: a revision of global budget estimates. *Global Biogeochemical Cycles* 22(2). doi:10.1029/2007GB003052.
- Childers, D.L., J.N. Boyer, S.E. Davis, C.J. Madden, D.T. Rudnick, and F.H. Sklar. 2006. Relating precipitation and water management to nutrient concentrations in the oligotrophic “upside-down” estuaries of the Florida Everglades. *Limnology and Oceanography* 51: 602–616.
- Christophersen, N., and R.P. Hooper. 1992. Multivariate analysis of stream water chemical data: the use of principal components analysis for the end-member mixing problem. *Water Resources Research* 28: 99–107. doi:10.1029/91WR02518.
- Christophersen, N., C. Neal, R.P. Hooper, R.D. Vogt, and S. Andersen. 1990. Modelling streamwater chemistry as a mixture of soilwater end-members—a step towards second-generation acidification models. *Journal of Hydrology* 116: 307–320. doi:10.1016/0022-1694(90)90130-P.
- Doctor, D., E.C. Alexander, M. Petriä, J. Kogoväjek, J. Urbanc, S. Lojen, and W. Stichler. 2006. Quantification of karst aquifer discharge components during storm events through end-member mixing analysis using natural chemistry and stable isotopes as tracers. *Hydrogeology Journal* 14: 1171–1191. doi:10.1007/s10040-006-0031-6.
- Eamus, D., and R. Froend. 2006. Groundwater-dependent ecosystems: the where, what and why of GDEs. *Australian Journal of Botany* 54: 91–96.
- Foster, S., and P. Chilton. 2003. Groundwater: the processes and global significance of aquifer degradation. *Philosophical Transactions of the Royal Society, Biological Sciences* 358: 1957–1972.

- Foster, D., F. Swanson, J. Aber, I. Burke, N. Brokaw, D. Tilman, and A. Knapp. 2003. The importance of land-use legacies to ecology and conservation. *Bioscience* 53: 77–88.
- Fourqurean, J.W., J.C. Zieman, and G.V.N. Powell. 1992. Relationships between porewater nutrients and seagrasses in a subtropical carbonate environment. *Marine Biology* 114: 57–65. doi:10.1007/BF00350856.
- Fourqurean, J.W., G.A. Kendrick, L.S. Collins, R.M. Chambers, and M.A. Vanderklift. 2012. Carbon, nitrogen and phosphorus storage in subtropical seagrass meadows: examples from Florida Bay and Shark Bay. *Marine and Freshwater Resources*. 63: 967–983.
- Frankovich, T.A., and R.D. Jones. 1998. A rapid, precise and sensitive method for the determination of total nitrogen in natural waters. *Marine Chemistry* 60: 227–234. doi:10.1016/S0304-4203(97)00100-X.
- Garrett, C. G., V. M. Vulava, T. J. Callahan, and M. L. Jones (2012). Groundwater–surface water interactions in a lowland watershed: source contribution to stream flow. *Hydrological Processes*. 3195, doi:10.1002/hyp.8257.
- Gondwe, B.R.N., S. Lerer, S. Stisen, L. Marín, M. Rebolledo-Vieyra, G. Merediz-Alonso, and P. Bauer-Gottwein. 2010. Hydrogeology of the south-eastern Yucatan Peninsula: new insights from water level measurements, geochemistry, geophysics and remote sensing. *Journal of Hydrology* 389: 1–17. doi:10.1016/j.jhydrol.2010.04.044.
- Gondwe, B.R.N., G. Merediz-Alonso, and P. Bauer-Gottwein. 2011. The influence of conceptual model uncertainty on management decisions for a groundwater-dependent ecosystem in karst. *Journal of Hydrology* 400: 24–40. doi:10.1016/j.jhydrol.2011.01.023.
- Halse, S., J. Ruprecht, and A. Pinder. 2003. Salinisation and prospects for biodiversity in rivers and wetlands of south-west Western Australia. *Australian Journal of Botany* 51: 673–688.
- Herrera-Silveira, J., I. Medina-Gomez, and R. Colli. 2002. Trophic status based on nutrient concentration scales and primary producers community of tropical coastal lagoons influenced by groundwater discharges. *Hydrobiologia* 475–476: 91–98. doi:10.1023/A:1020344721021.
- Herrera-Silveira, J.A., F.A. Comin, N. Aranda-Cirerol, L. Troccoli, and L. Capurro. 2004. Coastal water quality assesment in the Yucatan Peninsula: management implications. *Ocean and Coastal Management* 47: 625–639.
- Hooper, R.P., N. Christophersen, and N.E. Peters. 1990. Modelling streamwater chemistry as a mixture of soilwater end-members—an application to the Panola Mountain catchment, Georgia, U.S.A. *Journal of Hydrology* 116: 321–343. doi:10.1016/0022-1694(90)90131-G.
- Jensen, H.S., K.J. McGlathery, R. Marino, and R.W. Howarth. 1998. Forms and availability of sediment phosphorus in carbonate sand of Bermuda seagrass beds. *Limnology and Oceanography* 43: 799–810.
- Lachniet, M.S., and W.P. Patterson. 2009. Oxygen isotope values of precipitation and surface waters in northern central America (Belize and Guatemala) are dominated by temperature and amount effects. *Earth and Planetary Science Letters* 284: 435–446. doi:10.1016/j.epsl.2009.05.010.
- Lefticariu, M., E.C. Perry, W.C. Ward, and L. Lefticariu. 2006. Post-Chicxulub depositional and diagenetic history of the northwestern Yucatan Peninsula Mexico. *Sedimentological Geology*. 183: 51–69. doi:10.1016/j.sedgeo.2005.09.008.
- Lesser, J. 1976. Estudio hidrogeológico e hidrogeoquímico de la Península de Yucatan. Proyecto Conacyt-NSF 704:
- Liu, F., M. W. Williams and N. Caine. 2004. Source waters and flow paths in an alpine catchment, Colorado Front Range, USA. *Water Resources Research*. 40: W09401, doi:10.1029/2004WR003076
- Maher, D.T., I.R. Santos, L. Golsby-Smith, J. Gleeson, and B.D. Eyre. 2013. Groundwater-derived dissolved inorganic and organic carbon exports from a mangrove tidal creek: the missing mangrove carbon sink? *Limnology and Oceanography* 58(2): 475–488. doi:10.4319/lo.2013.58.2.0475.
- Marfia, A.M., R.V. Krishnamurthy, E.A. Atekwana, and W.F. Panton. 2004. Isotopic and geochemical evolution of ground and surface waters in a karst dominated geological setting: a case study from Belize, Central America. *Applied Geochemistry* 19: 937–946. doi:10.1016/j.apgeochem.2003.10.013.
- Medina-Gómez, I., and J.A. Herrera-Silveira. 2003. Spatial characterization of water quality in a karstic coastal lagoon without anthropogenic disturbance: a multivariate approach. *Estuarine, Coastal and Shelf Science* 58: 455–465. doi:10.1016/S0272-7714(03)00112-4.
- Metcalfe, C.D., P.A. Beddows, G.G. Bouchot, T.L. Metcalfe, H. Li, and H. Van Lavieren. 2011. Contaminants in the coastal karst aquifer system along the Caribbean coast of the Yucatan Peninsula Mexico. *Journal of Environmental Pollution*. 159: 991–997. doi:10.1016/j.envpol.2010.11.031.
- Middelburg, J., J. Nieuwenhuize, F. Slim, and B. Ohowa. 1996. Sediment biogeochemistry in an East African mangrove forest (Gazi Bay, Kenya). *Biogeochemistry* 34: 133–155. doi:10.1007/BF00000899.
- Moran, D. 2010. Carbon dioxide degassing in fresh and saline water. I: degassing performance of a cascade column. *Aquacultural Engineering* 43(1): 29–36.
- Murray, B.B.R., M.J.B. Zeppel, G.C. Hose, and D. Eamus. 2003. Groundwater-dependent ecosystems in Australia: it's more than just water for rivers. *Ecological Management and Restoration* 4: 110–113. doi:10.1046/j.1442-8903.2003.00144.x.
- Mutchler, T., K.H. Dunton, A. Townsend-Small, S. Fredriksen, and M.K. Rasser. 2007. Isotopic and elemental indicators of nutrient sources and status of coastal habitats in the Caribbean Sea, Yucatan Peninsula, Mexico. *Estuarine, Coastal and Shelf Science* 74: 449–457. doi:10.1016/j.ecss.2007.04.005.
- Olmsted, I. C., and R. Duran. 1990. Vegetacion de Sian Ka'an. In D. Navarro and J. Robinson [eds.], *Diversidad Biologica en Sian Ka'an*, Quintana Roo, Mexico. Programs for Studies in Tropical Conservation, University of Florida.
- Ovalle, A.R.C., C.E. Rezende, L.D. Lacerda, and C.A.R. Silva. 1990. Factors affecting the hydrochemistry of a mangrove tidal creek, Sepetiba Bay, Brazil. *Estuarine, Coastal and Shelf Science* 31: 639–650. doi:10.1016/0272-7714(90)90017-L.
- Parkhurst, D.L. and C.A.J. Appelo. 1999. User's guide to PHREEQC (version 2) - a computer program for speciation, reaction-path, 1Dtransport, and inverse geochemical calculations. *US Geological Survey Water Resources Investigation Report* 99-4259, 312p
- Perry, E., L. Marin, J. McClain, and G. Velazquez. 1995. Ring of Cenotes (sinkholes), northwest Yucatan, Mexico: its hydrogeologic characteristics and possible association with the Chicxulub impact crater. *Geology* 23: 17–20. doi:10.1130/0091-7613(1995)023<0017:ROCSNY>2.3.CO;2.
- Perry, E., G. Velazquez-Oliman, and L. Marin. 2002. The hydrogeochemistry of the karst aquifer system of the Northern Yucatan Peninsula Mexico. *International Geology Review*. 44: 191–221. doi:10.2747/0020-6814.44.3.191.
- Perry, E. M., G. Velazquez-Oliman, and R. A. Socki. 2003. Hydrogeology of the Yucatan Peninsula, p. 115–138. In A. Gomez-Pompa, M. F. Allen, S. L. Fedick and J. J. Jimenez-Osornio [eds.], *The Lowland Mayan Area: Three Millennia at the Human-Wildland Interface*. Food Products Press.
- Perry, E., A. Paytan, B. Pedersen, and G. Velazquez-Oliman. 2009. Groundwater geochemistry of the Yucatan Peninsula Mexico: constraints on stratigraphy and hydrogeology. *Journal of Hydrology* 367: 27–40. doi:10.1016/j.jhydrol.2008.12.026.
- Perry, E. C., Velazquez-Oliman, G., and Wagner, N. 2011. Preliminary investigation of groundwater and surface water geochemistry in Campeche and southern Quintana Roo. In *Water Resources in México: Scarcity, Degradation, Stress, Conflicts, Management and Policy*. Ursula Oswald Spring Ed. Springer-Verlag. 522p. pp 87–97

- Pope, K. O., A. C. Ocampo, A. G. Fischer, F. J. Vega, D. E. Ames, D. T. King, B. W. Fouke, R. J. Wachtman, and G. Kletetschka (2005). Chicxulub impact ejecta deposits in southern Quintana Roo, Mexico, and central Belize, p. 171. In T. Kenkman, F. Horz and A. Deutsch [eds.], Large meteorite impacts III. Geological Society of America.
- Price, R.M., P.K. Swart, and J.W. Fourqurean. 2006. Coastal groundwater discharge—an additional source of phosphorus for the oligotrophic wetlands of the Everglades. *Hydrobiologia* 569: 23–26.
- Rejmánková, E., and J. Komárková. 2000. A function of cyanobacterial mats in phosphorus-limited tropical wetlands. *Hydrobiologia* 431: 135–153. doi:10.1023/A:1004011318643.
- Rezaei, M., E. Sanz, E. Raeisi, C. Ayora, E. Vázquez-Suñé, and J. Carrera. 2005. Reactive transport modeling of calcite dissolution in the fresh-salt water mixing zone. *Journal of Hydrology* 311: 282–298. doi:10.1016/j.jhydrol.2004.12.017.
- Salinas-Prieto, J. C., J. M. Escobar, E. Sanchez-Rojas, C. Diaz-Salgado, A. de la Calleja, D. Barajas-Nigoche, and E. Salgado-Dorantes. 2007. Carta geológica de México
- Sanford, W. E. and L. F. Konikow. 1989. Porosity development in coastal carbonate aquifers. *Geology*. 17: 249–252, doi:10.1130/0091-7613(1989)017<0249:PDICCA>2.3.CO;2.
- Santos, I.R., R.N. Peterson, B.D. Eyre, and W.C. Burnett. 2010. Significant lateral inputs of fresh groundwater into a stratified tropical estuary: evidence from radon and radium isotopes. *Marine Chemistry* 121: 37–48. doi:10.1016/j.marchem.2010.03.003.
- Sherman, R.E., T.J. Fahey, and R.W. Howarth. 1998. Soil-plant interaction in neotropical mangrove forest: Iron, phosphorus and sulfur dynamics. *Oecologia* 115: 553–563.
- Short, F., W. Dennison, and D. Capone. 1990. Phosphorus-limited growth of the tropical seagrass *Syringodium filiforme* in carbonate sediments. *Marine Ecology Progress Series* 62: 169–174.
- Smart, P.L., J.M. Dawans, and F. Whitaker. 1988. Carbonate dissolution in a modern mixing zone. *Nature* 335: 811–813.
- Solórzano, L., and J.H. Sharp. 1980. Determination of total dissolved phosphorus and particulate phosphorus in natural water. *Limnology and Oceanography* 24(4): 754–758. doi:10.4319/lo.1980.25.4.0754.
- Taylor, R., B. Kelbe, S. Haldorsen, G. Botha, B. Wejden, L. V. Året, and M. Simonsen. 2006. Groundwater-dependent ecology of the shoreline of the subtropical Lake St Lucia estuary. *Environmental Geology* 49: 586–600. doi:10.1007/s00254-005-0095-y.
- Valdes, D.S., and E. Real. 2004. Nitrogen and phosphorus in water and sediments at Ria Lagartos coastal lagoon, Yucatan Gulf of Mexico. *Indian Journal of Marine Sciences*. 33: 338–345.
- Vervier, P., L. Roques, M. A. Baker, F. Garabetian and P. Auriol. 2002. Biodegradation of dissolved free simple carbohydrates in surface, hyporheic and riparian waters of a large river. 153: 595–604.
- Vulava, V. M., C. G. Garrett, C. L. Ginn and T. J. Callahan. 2008. Application of geochemical end-member mixing analysis to delineate water sources in a lowland watershed. Proceedings of the 2008 South Carolina Water Resources Conference. 1–4
- Ward, W.C. 1985. Quaternary geology of northeastern Yucatán Peninsula. In *Geology and hydrogeology of Northeastern Yucatán and Quaternary Geology of Northeastern Yucatan*. 23–95, ed. W.C. Ward, A.E. Weidie, and W. Back, 23–95. New Orleans, LA: New Orleans Geological Society.
- Ward, W.C., G. Keller, W. Stinnesbeck, and T. Adatte. 1995. Yucatán subsurface stratigraphy: implications and constraints for the Chicxulub impact. *Geology* 23: 873–876. doi:10.1130/0091-7613(1995)023<0873:YNSSIA>2.3.CO;2.
- Wigley, T.M.L., and L.N. Plummer. 1976. Mixing of carbonate waters. *Geochimica et Cosmochimica Acta* 40: 989–995. doi:10.1016/0016-7037(76)90041-7.
- Zaldívar-Jiménez, M.A., J.A. Herrera-Silveira, C. Teutli-Hernández, F.A. Comín, J.L. Andrade, C.C. Molina, and R.P. Ceballos. 2010. Conceptual framework for mangrove restoration in the Yucatán Peninsula. *Ecological Restoration. Ecological Restoration*. 28(3): 333–342.
- Zapata-Rios, X., and R.M. Price. 2012. Estimates of groundwater discharge to a coastal wetland using multiple techniques: Taylor Slough, Everglades National Park USA. *Hydrogeology*. 20: 1651–1668.
- Zhang, J., and X. Huang. 2011. Effect of temperature and salinity on phosphate sorption on marine sediments. *Environmental Science and Technology* 45: 6831–6837. doi:10.1021/es200867p.